



Northern fur seals augment ship-derived ocean temperatures with higher temporal and spatial resolution data in the eastern Bering Sea



Chad A. Nordstrom^{a,b,*}, Kelly J. Benoit-Bird^c, Brian C. Battaile^a, Andrew W. Trites^{a,b}

^a Marine Mammal Research Unit, Fisheries Centre, University of British Columbia, AERL, 2202 Main Mall, Vancouver, BC, Canada V6T 1Z4

^b Department of Zoology, University of British Columbia, #2370–6270 University Boulevard, Vancouver, BC, Canada V6T 1Z4

^c College of Earth, Ocean, and Atmospheric Sciences, Oregon State University, 104 CEOAS Administration Building, Corvallis, OR 97331, USA

ARTICLE INFO

Available online 19 March 2013

Keywords:

Bio-logging
Spatial interpolation
Data-interpolating variational analysis
Northern fur seal
Callorhinus ursinus
USA
Alaska
Eastern Bering Sea

ABSTRACT

Oceanographic data collected by marine vertebrates are increasingly being used in biological and physical studies under the assumption that data recorded by free-ranging animals are comparable to those from traditional vertical sampling. We tested this premise by comparing the water temperatures measured during a 2009 oceanographic cruise with those measured during 82 foraging trips by instrumented northern fur seals (*Callorhinus ursinus*) in the eastern Bering Sea. The animal-borne data loggers were equipped with a fast-response temperature sensor and recorded 6492 vertical profiles to depths ≥ 50 m during long distance (up to 600 km) foraging trips. Concurrent sampling during the oceanographic cruise collected 247 CTD casts in the same 5-week period. Average temperature differences between ship casts and seal dives (0.60 ± 0.61 °C), when the two were within 1 day and 10 km of each other ($n=32$ stations), were comparable to mean differences between adjacent 10 km ship casts (0.46 ± 0.44 °C). Isosurfaces were evaluated at region wide scales at depths of 1 m and 50 m while the entire upper 100 m of the water column was analyzed at finer-scales in highly sampled areas. Similar patterns were noted in the temperature fields produced by ships or seals despite the differences in sampling frequency and distribution. However, the fur seal dataset was of higher temporal and spatial resolution and could therefore be used to visualize finer detail with less estimated error than ship-derived data, particularly in dynamic areas. Integrating the ship and seal datasets provided temperature maps with an unprecedented combination of resolution and coverage allowing fine-scale processes on-shelf and over the basin to be described simultaneously. Fur seals ($n=65$ trips) also collected 4700 additional profiles post-cruise which allowed ≥ 1 °C warming of the upper 100 m to be documented through mid-September, including regions where ship sampling has traditionally been sparse. Our data show that hydrographic information collected by wide-ranging, diving animals such as fur seals can contribute physical data comparable to, or exceeding those, of traditional sampling methods at regional or finer scales when the questions of interest coincide with the ecology of the species.

© 2013 Elsevier Ltd. All rights reserved.

1. Introduction

Traditional oceanographic sampling has been increasingly supplemented with data collected by free-ranging marine vertebrates (Biuw et al., 2007; Boyd et al., 2001; Charrassin et al., 2002; Lydersen et al., 2004; Roquet et al., 2009; Simmons et al., 2010). Animal-borne sensors have gathered large numbers of high-resolution vertical profiles over wide areas and long time periods but with an inherently different sampling strategy than the

regularized data collection protocols (e.g. transects) generally used by ships, moorings or satellites. Despite temporal and spatial differences in sampling, oceanographic data collected by animals have contributed to models of ocean heat flux, predictions of frontal strength, and deep-water turnover estimates (Boehme et al., 2008; Charrassin et al., 2008; Costa et al., 2008; Grist et al., 2011). Technical validations of the tags have been performed in the field and the lab (Roquet et al., 2011; Simmons et al., 2009), but to date there have been no large scale comparisons of data derived from *in-situ* platforms employing standard data collection techniques with those from animal-borne instruments sampling according to highly individualized spatiotemporal use. Animal-borne sensors can be powerful tools to collect habitat data, but only if the data can be assumed to be, at minimum, comparable to habitat descriptions previously obtained from more

* Corresponding author. Tel.: +1 604 822 6557; fax: +1 604 822 8180.

E-mail addresses: c.nordstrom@fisheries.ubc.ca (C.A. Nordstrom), b.battaile@fisheries.ubc.ca (K.J. Benoit-Bird), kbenoit@coas.oregonstate.edu (B.C. Battaile), a.trites@fisheries.ubc.ca (A.W. Trites).

traditional ocean profiling techniques, and this has yet to be examined on a large scale.

The eastern Bering Sea is a hydrographically complex region north of the Aleutian arc comprising a broad, shallow (<200 m) continental shelf with a deep oceanic basin (>3000 m) separated by a narrow shelf break (Fig. 1). The region is a seasonally productive high-latitude system where the coupling of physical and biological processes supports large aggregations of sea-birds and marine mammals (Hunt Jr. and Stabeno, 2002; Sinclair et al., 2008). Well described temperature domains at the mesoscale are defined by the major isobaths, although at the sub-mesoscale (<10 km) conditions can be highly dynamic (Stabeno et al., 2001, 2008; Sullivan et al., 2008). For example, the middle continental shelf (50 to <100 m) typically consists of two well-structured temperature layers compared to the three diffuse layers on the outer shelf (100 to <200 m) with the transition between the two relatively coincident with the 100 m isobaths. In addition, a bottom layer of water <2 °C (cold-pool) remnant from sea ice melt occupies the middle-shelf, but its extent shifts inter-annually (Stabeno et al., 2001). Eddies, meanders of the major northward currents, and disturbances created by bottom topography all introduce fine-scale variability within the region's large expanse (Ladd et al., 2012; Okkonen et al., 2004; Schumacher and Stabeno, 1994; Stabeno and van Meurs, 1999).

Northern fur seals (*Callorhinus ursinus*) are apex predators in the Bering Sea with an ecology that makes them well-suited

platforms for fine-scale sampling across varied habitats and large distances. These small otariids return from the open North Pacific to islands in the Bering Sea to breed, give birth and rear pups for 4 months each summer. During this period, lactating females intersperse wide-ranging (up to 600 km) foraging trips at-sea with nursing bouts ashore (Gentry, 1998). As a result, complete data records can be recovered following foraging trips instead of necessitating the use of sub-sampled data typically relayed through satellites, thereby facilitating examination of fine-scale oceanographic data from complex environments. Lactating northern fur seals also employ multiple foraging strategies (Goebel et al., 1991) and exhibit a large degree of inter-individual difference in terms of where animals travel in search of prey. While females appear to show some fidelity to areas where they previously foraged (Call et al., 2008; Robson et al., 2004), they do not appear to target specific foraging grounds as commonly seen in other species (e.g., Campagna et al., 2001; Chilvers et al., 2005; Lea et al., 2008; Trathan et al., 2006; Weise et al., 2010). From a sampling perspective, the routes used by the fur seals appear almost random at the island population level. This fine-scale heterogeneous sampling, in conjunction with their wide-ranging movements and predictable returns to the rookery for instrument recovery, should make the northern fur seal an excellent animal platform from which to study the physical parameters of the eastern Bering Sea. Reciprocally, a greater understanding of

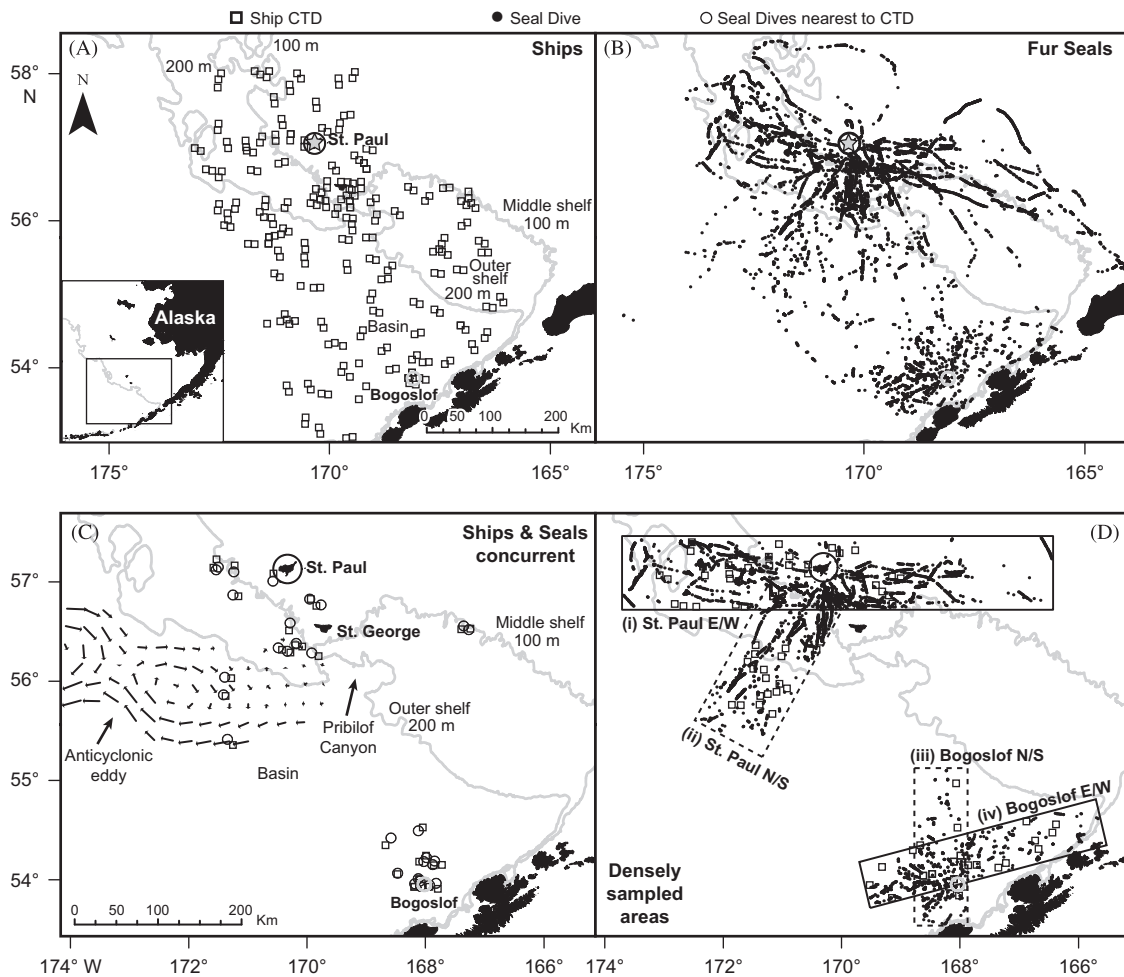


Fig. 1. Sampling stations with ocean temperature profiles ≥ 50 m in the eastern Bering Sea: (A) ship CTD casts ($n=247$) from July 18 to August 14, 2009; (B) fur seal dives from July 15 to September 17, 2009 ($n=11,192$); (C) concurrent CTD casts (open squares) and seal dives (open circles) within 10 km and 1 day of each other ($n=32$); and (D) delineated sub-regions where ships (open squares) and seals (black circles) sampled most frequently. The 200 m isobaths marks the approximate location of the shelf-break dividing the Bering Sea basin (west) from the continental shelf (east).

fine-scale oceanography could lead to insights into the ecology of the northern fur seal (e.g., Nordstrom et al., 2012; Sterling, 2009).

The overall objective of the study was to compare the upper water temperatures collected by ships with similar data collected by northern fur seals in the eastern Bering Sea. More specifically, we deployed fast-response temperature sensors (thermistors) on 31 northern fur seals concomitantly with ship-board sampling designed to support ecological studies of upper trophic predators. This provided a unique opportunity to collect point-sampled oceanographic data from different platforms operating independently and simultaneously over the same geographical region. Not only could the information be compared to examine differences between ship and fur seal collections but the data could also be combined to describe the oceanography of the region more completely. Our goals were to (1) compare water temperatures measured during a 2009 oceanographic cruise with those from instrumented fur seals, (2) evaluate interpolated temperature maps derived from each data source, and (3) describe summer conditions in the eastern Bering Sea using the novel, integrated dataset.

2. Materials and methods

2.1. Ship sampling

The goal of the sampling program was to describe the distributions and habitat conditions of forage fish and krill that were likely to support upper predators such as fur seals and seabirds from colonies in the eastern Bering Sea during the summer. The survey was therefore designed to collect data within 200 km of the Pribilof Islands and 200 km north–northwest of Bogoslof Island where major colonies were located to examine the consequences of variation in prey and oceanography on the at-sea distribution of predators. The area between St. Paul Island (57.1°N, 170.3°W) and Bogoslof Island (53.9°N, 168.0°W) was sampled from July 18th to August 14th, 2009 from chartered fishing vessels (the 43 m FV 'Frosti' and the 32 m FV 'Goldrush'). Prey sampling consisted of a series of 10 km long transects (trawls) and physical oceanographic sampling consisted of paired stations at the beginning and end of each transect. A total of 247 stations were distributed over three, hydrographically distinct zones (Coachman, 1986): middle shelf with bottom depths between 50 and 100 m (45 stations); outer shelf with bottom depths between 100 and 200 m (81 stations); and slope/basin with depths greater than 200 m (121 stations) (Benoit-Bird et al., 2011). The first station in each pair was randomly located as was the orientation to the next station. Transects were not allowed to cross region boundaries or other transects (Fig. 1A). Note that odd numbers of stations represent data loss from individual instrument deployments but at least one profile was collected for each transect.

A CTD (conductivity, temperature, and depth) profile was conducted at each station (at the beginning and end of each 10-km transect). A Sea-Bird SBE19plus CTD was guided by a real time remote pressure sensor (Simrad PI60) and lowered to a depth of 100 m or 5 m from the bottom if the sea floor was < 100 m from the surface. Each CTD was also equipped with a dissolved oxygen sensor, a transmissometer within the visible spectrum for most fish, and a fluorometer. Data were low pass filtered, aligned to account for instrument lags, and edited for loops (to account for ship heaving) before the raw data were converted to variables of interest using factory calibrations.

2.2. Seal sampling

Lactating fur seals at St. Paul Island (Reef rookery, $n=44$ females) and Bogoslof Island ($n=43$ females) were instrumented

with Mk10-F GPS enabled time-depth recorders equipped with fast-response thermistors (Wildlife Computers, WA, USA) from July 11th to September 19th, 2009. Each GPS tag ($102 \times 60 \times 31 \text{ mm}^3$) was paired with a VHF transmitter ($45 \times 31 \times 15 \text{ mm}^3$) to assist with instrument recovery (Advanced Telemetry Systems, MN, USA). The archival Mk10-F tags recorded depth (0.5 m resolution), external temperature (0.52 s response, 0.05 °C resolution, 0.1 °C accuracy, Hill pers. comm.), and light level once per second. Fastloc™ GPS fixes were attempted every 15 min while the animal was at the surface.

Females on St. Paul Island were tagged at Reef rookery because fur seals from this location have been shown to forage in all hydrographic domains around the island (Robson et al., 2004). Instruments were deployed on fur seals from 3 rookeries on Bogoslof Island with different geographic orientations to ensure tracks were representative for the island. Seals were captured using a mobile blind (July) or via hoop-net (August–September). Individual females were chosen based on size and the presence of a healthy pup and/or adequate milk production. These criteria increased the likelihood that females would return to the rookery for instrument recovery and redeployment. Animals were physically restrained using custom restraint-boards and neoprene wraps to allow devices to be glued to the dorsal pelage along the seal's midline using 5-min epoxy (Devcon®, MA, USA). Hoop-netted females were weighed (± 0.1 kg, mean=39.2 kg) using an MSI-7200 Dyna-Link digital scale (Measure Systems International, Seattle, WA). Standard lengths (± 1 cm, mean=121.4 cm) and girths (± 1 cm, mean=81.1 cm) were also measured whenever possible for all animals but were generally more challenging to obtain from the mobile blind. Animals were recaptured, physically restrained, re-measured, and devices were removed following foraging trips (deployment interval=5–39 days, mean=14 d). Capture teams based on each island redeployed instruments on successive animals after the data were recovered to increase the sample size of tagged individuals.

Profiles collected from fur seals were divided into 2 time periods: (1) July 15–August 15 (to match the ship cruise), and (2) from August 16 to September 17 (post-cruise until the last profile). The tag's salt-water switch was used to determine the start and end of each foraging trip in conjunction with GPS fixes. GPS locations were filtered to remove points requiring unlikely average travel speeds (> 3 m/s) by calculating the running mean of speed using the previous and next locations for each fix. Tracks were linearly interpolated between points as temporal resolution was generally very high (mean=17.4 post-filtered locations per day) (Tremblay et al., 2006). GPS points were rarely removed (99% of at-sea locations were retained) and those that were eliminated tended to be gross anomalies (e.g., basin wide movements within hours).

Dive data were zero-offset corrected using Wildlife Computer's DAP program (v.2.063) with dives defined as those reaching at least 5 m. Each dive was enumerated and broken into descent, bottom, or ascent portions using 80% of the maximum dive depth as the transition points. Maximum depth (m) was recorded and dives > 50 m were retained for comparison with ship profiles. Locations for the start and end of each dive were determined by matching the dive times to the interpolated track via the tag's clock (Fig. 1B).

The Mk10 external temperature data were processed according to validations conducted by Simmons et al. (2009). Briefly, external temperature readings were aligned with the depth sensor by applying a 1-s time lag and corrected by subtracting 0.05 °C. Seal dives were binned at 1-m intervals and temperature values were interpolated using a hermite spline. As most seals dived at < 1 m/s, temperature measures were averaged more often than interpolated for a given depth.

2.3. Satellite altimetry

Supplementary data describing the positions of mesoscale eddies and other submesoscale fronts over the basin on July 29 were also considered. These data provided a snapshot of frontal activity at the mid-point of the composite temperature maps and provided context for the patterns observed over the basin. Maps of sea-surface height (SSH) and geostrophic current anomalies were created from merged, delayed-time (corrected) satellite altimetry distributed by Aviso, France (<http://www.aviso.oceanobs.com>). The positions of fine-scale fronts were then estimated from 4-day maps of surface Lagrangian coherent structures (e.g. transport barriers, filament edges, or eddy boundaries). These 4-day maps were in turn derived from the geostrophic current anomalies using the finite-size Lyapunov exponent (FSLE) method which is well suited to study the properties of transport in fluid flow (Boffetta et al., 2001; d'Ovidio et al., 2004). Low FSLE values coincide with areas of low dispersion rates (e.g. eddy cores) while regions of large Lyapunov exponents are associated with areas of high dispersion such as the outer part of eddies and strong fronts (d'Ovidio et al., 2004; Resplandy et al., 2009). We contoured the FSLE values at 0.2 FSLE/d to reproduce the edges of the strongest fronts which was suitable for comparison with the aggregated temperature data.

2.4. Creation of datasets

Composite temperature maps for the study region were created by gridding the point-sample data collected by ships and seals. All maps of isosurfaces and vertical cross-sections were interpolated using the data-interpolating variational analysis (DIVA) method (Brasseur et al., 1996; Rixen et al., 2000; Troupin et al., 2010) as implemented in the Ocean Data View (v.4.4.2) software package (Schlitzer, 2011a, <http://odv.awi.de>). The DIVA algorithm is akin to optimal interpolation techniques but incorporates directional constraints and barriers such as bottom topography. Any re-created field is sensitive to correlation length (the range over which fluctuations in one region of space influence those in another) and, as with other gridding algorithms, the smoothness of the estimated field is controlled by adjusting the correlation length (Schlitzer, 2011b). Larger values allow for the assimilation of data from points further apart and result in smoother fields but at the expense of potentially losing fine-scale detail. The correlation length is set as the percent of x (e.g. longitude) and y or z (e.g. latitude or depth) in Ocean Data View therefore the areal extent of each surface was fixed prior to gridding. For example, we set a correlation length of 1% over a depth range of 110 m for all cross-sections to consistently allow each sample to influence the gridded value of vertically neighboring samples out to 1.1 m. Correlation lengths are reported as percentages with their equivalent linear distance in km.

2.4.1. Maps of isosurfaces

Separate temperature isosurfaces were generated from data collected across the region by ships or by seals for the area covering 174.25–164.0°W by 58.75–53.25°N using Ocean Data View at the default projection. Maps were created at 1 m and 50 m depth slices. This allowed us to estimate temperature at layers routinely sampled by both platforms across the entire sampling region. The 1 m depth slice was specifically chosen as a proxy for sea-surface temperature (SST) so it could be used as a stand-alone product for a region subject to extensive, satellite obscuring cloud cover while also easing potential comparison with other studies of marine predators that make use of satellite derived SST. The 50 m slice was chosen as it allowed us to

describe temperatures in a relatively less variable layer and use fur seal dives across the region as they rarely dove > 50 m when over the Bering Sea basin.

Datasets were later merged and isosurfaces at 1 and 50 m were again produced using integrated data from ships and seals. This allowed us to describe the eastern Bering Sea using all available data for the period of July 15–August 15. All isosurface maps were generated using a conservative correlation length of 1.3% (7.5 km latitude \times 8.3 km longitude) which was based on the 10 km separation between nearest ship casts.

2.4.2. Vertical cross-sections

Finer spatial scale cross-sections were interpolated from complete CTD profiles and from entire fur seal dives in sub-regions that were sampled most often (Fig. 1D) during 6-week blocks. This allowed us to examine the variability of the water column in highly sampled regions as described by either platform and to examine seasonal changes in temperature between two time-periods using data collected by the fur seals. Vertical cross-sections were generated using either 1% of longitude (3.0 km, sub-region i) or 2% (4.4 km, sub-region ii–iv) of latitude/longitude depending on the sampling density. Correlation length was kept consistent for ship and seal data within a sub-region and a correlation length of 1% (1.1 m) was used for depth in all cross-sections.

2.4.3. Error fields

The spatial distribution of analysis error is of interest when estimating a continuous spatial field in that it provides a relative measure of where one can have more or less confidence in the resulting map. Briefly, the analysis (DIVA interpolation) was applied on a vector containing the covariances of the data locations where the error needed to be calculated. DIVA, as enabled within Ocean Data View, employed a basic or poor man's error field (Barth et al., 2010; Troupin et al., 2010) which substituted a vector of values with constant variance for calculations performed by the analyzed field. This allowed the error to be assessed in all locations with the same analysis which in turn allowed for relatively rapid computation at the expense of underestimating true error (Troupin et al., 2012). As such, the error maps produced in these analyses should be considered minimum estimates of total error.

Errors estimates produced for the interpolated temperature fields incorporated instrument error (inherently as the values are considered anomalies against a constant background field) and sampling distribution error. Ocean Data View used the error estimates to restrict mapping to areas with error values below a user defined tolerance. The default quality limit of 0.25 was used as it produced relatively contiguous temperature maps without extrapolating estimates beyond the sampling region (errors are presented as the standard deviation relative to the field variance). This created irregularly shaped temperature maps and often produced "gaps" within isosurfaces/cross-sections but it retained only those estimates with errors below the defined threshold. The poor man's error field can be considered an efficient way to assess data coverage and determine which regions of the analysis cannot be trusted, however; other detailed analyses (such as the creation of climatologies) should make use of alternative methods to generate less optimistic error fields (Troupin et al., 2012).

2.5. Analysis techniques

2.5.1. Comparing in-situ temperatures

Temperatures from CTD casts and the corresponding nearest seal dives were directly compared at 1, 25, 50, 75, and 100 m

(as dives permitted) when they co-occurred within 10 km and 24 h (Fig. 1C). Previous, side-by-side validations have shown good agreement between the thermistor in the Mk10 and CTD sensor (Simmons et al., 2009). Temperature values from data-loggers were regressed against CTD values at paired depths and summary statistics were calculated for absolute differences using the R software package (R Development Core Team, 2009). All reported values include \pm standard deviation unless otherwise noted.

2.5.2. Comparing temperature isosurfaces

We compared maps of isosurfaces in 5 specific ways by (1) qualitatively assessing broad temperature patterns, (2) quantitatively examining fits and errors within surfaces (two methods), and (3) quantitatively comparing interpolated values between surfaces (two methods).

First, regional temperature maps were examined visually to assess how features such as the cold pool and transitions along the isobaths compared between maps produced from ship or seal data. Second, we measured the quality of each interpolated surface via cross-correlation (estimated goodness of fit) using *a priori* estimates of correlation length and signal-to-noise ratio generated by the DIVA fit routine (Barth et al., 2010). Third, error estimates obtained for individual surfaces from Ocean Data View were mapped using ArcGIS 9.3.1 software for additional within surface assessment.

Fourth, we directly compared temperature/error estimates extracted from ship and seal isosurfaces at 1 km intervals along a 300 km transect across the continental shelf (173.35–166.0°W at 51.1°N) and along a 235 km transect from the basin across the shelf-break to St. Paul Island (55.5–57.1°N; 172.0–170.3°W). Extracted transects were placed along the mid-line of densely sampled sub-regions (Fig. 1D). Fifth, regional surface maps were contrasted using a difference surface and a normalized difference surface for each depth slice that we generated by overlaying the ship derived field on the seal derived field and subtracting them. The normalized difference surface examined where differences between the fields was larger than the estimated errors and was defined as:

$$\text{Normalized difference} = \frac{\text{Ship temperature} - \text{Seal temperature}}{\sqrt{(\text{ship error}^2 + \text{seal error}^2)}} \quad (2.1)$$

where ship error and seal error are the standard deviations relative to the field variance of the respective surfaces.

2.5.3. Comparing vertical sections

Difference cross-sections were created from seal derived data for each of the 4 sub-regions by overlaying fields from July–August 15 with those from August 15–September and subtracting their gridded values. We calculated the standard deviation of the gridding errors over the section and doubled that value (2x SD) to obtain a threshold above which any temperature changes were likely to reflect actual differences between time periods as opposed to artifacts of the gridded interpolation. Further summary statistics on smaller patches within the difference section were calculated in Ocean Data View.

3. Results

3.1. Ship sampling

Temperatures ranged from -0.10 °C (measured in the cold-pool to the north-east of St. Paul Island) to 10.57 °C (measured at 1 m along the shelf break to the south-west of St. Paul Island). While stations were selected randomly within the study area, they were relatively well distributed at the regional scale (Fig. 1A) compared to the clumped, non-random distribution exhibited by the fur seals (Fig. 1B). The delineated sub-regions in Fig. 1D

covered 30.8% of the area sampled by ships and incorporated 36% of all ship casts, further highlighting the relatively even spatial sampling achieved by the ships within the study region.

3.2. Seal sampling

St. Paul Island ($n=44$) and Bogoslof Island ($n=41$) fur seals completed 147 foraging trips (July–August, $n=82$; August–September, $n=65$) recording at least one 50 m temperature profile (Table S1). Fur seals collected 11,192 profiles to depths ≥ 50 m during foraging dives at-sea between July 15th and September 17th, 2009 (July–August, $n=6492$; August–September, $n=4700$; Fig. 1B). Recorded temperatures ranged from -0.80 °C (in the cold pool east of St. Paul Island) to 10.45 °C (in the 1 m surface waters along the 100 m isobath south-east of St. Paul Island).

Profiles were collected relatively evenly between the middle domain ($n=3497$), the outer domain ($n=4060$), and the slope/basin ($n=3635$) of the eastern Bering Sea. Dives were nonetheless clumped within regions as the sub-regions delineated in Fig. 1D encompassed 21.6% of the area sampled by fur seals yet incorporated 50.9% of all sampling dives > 50 m.

St. Paul Island fur seals foraged widely as expected, radiating in all directions from the island with a notable concentration of southward trips. Seals originating from St. Paul Island traveled farther, were at-sea longer, and dove > 50 m more regularly (Nordstrom et al., 2012) and in doing so collected more profiles ($n=9325$) than seals from Bogoslof Island ($n=1867$). Some trips from St. Paul Island were restricted to the continental shelf and sampled the middle and outer shelf domains only while trips that reached the basin sampled all three hydrographic zones as they had to cross the shelf to reach the slope and basin regions.

Bogoslof Island fur seals did not pass through the Aleutian island chain but constrained their foraging trips primarily to the Bering Sea basin with occasional dives along the continental margins. Fewer sampling dives, generally restricted to the basin or slope regions, were recorded despite the greater number of trips performed by fur seals from Bogoslof Island. This was to be expected given Bogoslof Island's location over the basin when coupled with their shorter trips and their propensity for shallow diving (Nordstrom et al., 2012).

3.3. Comparing in-situ temperature

Seal dives ≥ 50 m coincided spatially and temporally with ship-borne CTD casts (within 10 km and 24 h of each other) on 48 occasions. Of these, 32 unique casts were directly compared to the nearest seal dive (Fig. 1C) as depths permitted (e.g. Fig. 2). Overall there was good agreement between paired ship casts and seal dives (e.g. Fig. 2A–C) when comparing absolute temperature differences at pre-determined depths (median=0.32, mean= 0.60 ± 0.61 °C). Differences were comparable to sequential CTD casts (within 10 km of each other) at those same depths ($n=120$ pairs, median=0.36 median, mean= 0.46 ± 0.44 °C)

Regression analysis of paired temperature values ($n=87$ pairs) showed significant correlations between values recorded from either platform ($F_{1,85}=516.1$, $p < 0.001$, adj. $R^2=0.87$; Fig. 3) and confidence intervals (95%) showed little uncertainty about predicted values. Most points were within 0.6 °C (the mean absolute difference between temperature pairings) of predicted values, particularly when temperatures were < 4 and > 8 °C which was typical of stable water masses well below or above the thermocline respectively.

3.4. Comparing temperature isosurfaces

Each of the five different methods used to compare interpolated temperature surfaces illustrated that those created from the

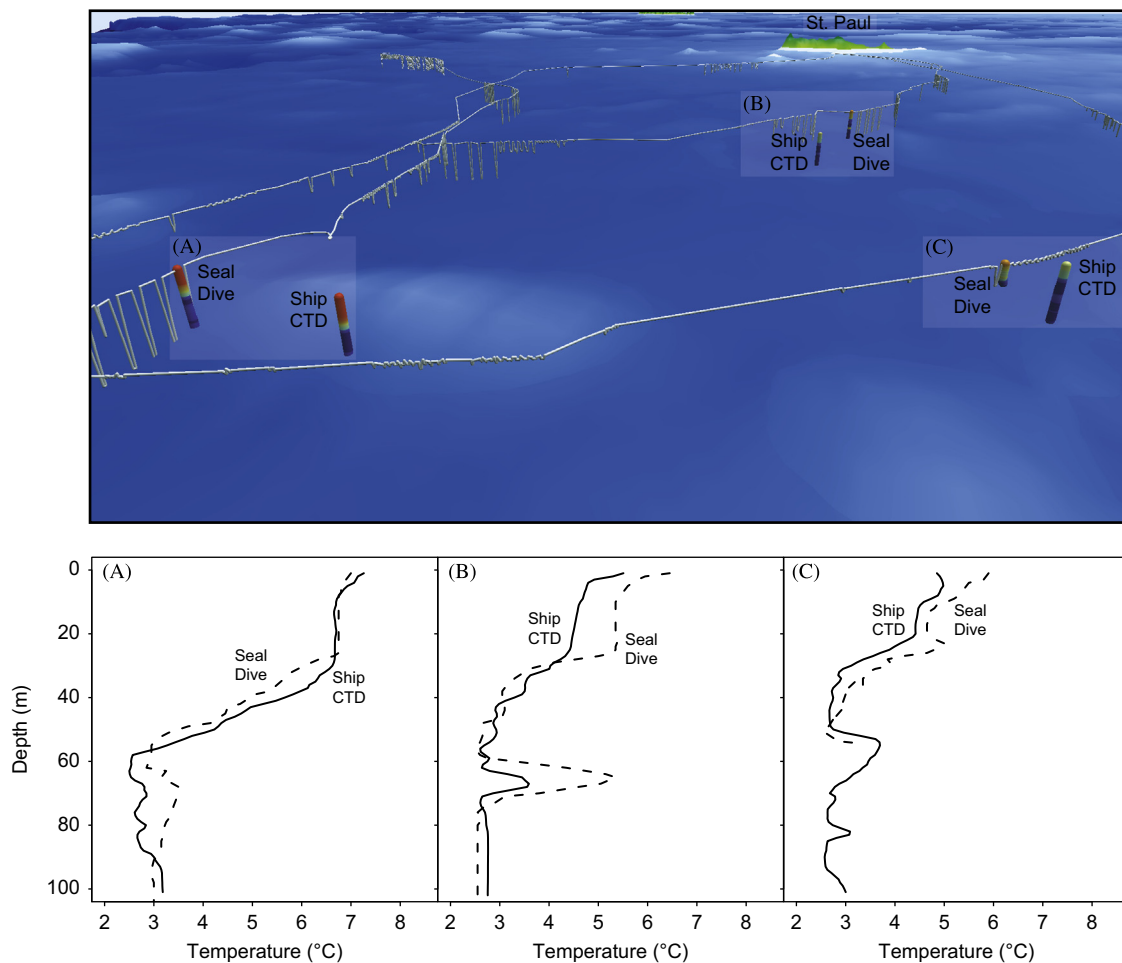


Fig. 2. Examples of paired temperature profiles collected by concurrent ship CTD casts and instrumented northern fur seals when sampling occurred within 10 km and 24 h. The upper panel depicts 3 pairs of *in-situ* profiles (colored vertical lines) on the continental shelf south of St. Paul I. White lines: fur seal surface track and additional dives. The lower panels compare the temperature-depth profiles from each ship cast (solid lines) and fur seal dive (dashed lines) pairing respectively (A: Dive SP09-0207 vs. CTD-34; B: Dive SP04B-0072 vs. CTD-32; C: Dive SP06-1466 vs. CTD-36).

seal data were equivalent or exceeded those produced from ship data in terms of areal coverage, detail, or quality.

3.4.1. Qualitative comparisons

Seal derived temperature fields at depths of 1 m and 50 m were qualitatively very similar to fields generated by standard CTD profiling despite obvious differences in the extents of the areas sampled (Fig. 4). The CTD data provided a nearly contiguous surface from north of St. Paul Island to south of Bogoslof Island thanks to the relatively even distribution of sampling stations over the study area. In contrast, seal surfaces were irregularly shaped polygons as they were generated from clumped sampling dives restricted along widely dispersed foraging tracks. While we did not detect any overlap in the foraging areas between the two different fur seal populations (St. Paul Island and Bogoslof Island), a sufficient number of sampling dives existed along the periphery of each fur seal range to bridge the surface into a collective whole rather than generating disjointed maps around each island. Instrumented seals provided highly detailed temperature data over a large expanse of the eastern Bering Sea with the early summer surfaces (Fig. 4C and D) providing more coverage over the continental shelf east of the Pribilofs while later summer surfaces were more contiguous over the basin (Fig. 4E and F).

Isosurfaces from both ships and seals highlighted similar features at the regional scale including cooler waters ($\sim 3\text{--}4\text{ }^{\circ}\text{C}$) surrounding the Pribilof Islands' at 1 m depth from July through August (Fig. 4A and C). They also delineated the cold-pool (waters $< 2\text{ }^{\circ}\text{C}$) north and east of the archipelago at 50 m although seals did not sample north of St. Paul Island until late August (Fig. 4F). Both data collection platforms also revealed a band of cool water ($\sim 2.5\text{ }^{\circ}\text{C}$; light-blue in Fig. 4) extending along the 100 m isobath across the outer shelf south and west of St. George Island.

Seal derived temperature surfaces showed greater spatial variability than ship derived surfaces and revealed finer scale heterogeneity of temperature within areas both on and off the continental shelf (Fig. 4A–D). For example, the large numbers of samples taken on the shallow plateau between St. Paul and St. George Islands showed that well-mixed waters at 1 m surrounded and connected both islands despite intrusions of warmer surface waters. Seals also revealed greater temperature fluctuations along the 100 and 200 m isobaths (particularly around the Pribilof Canyon) as well north and west of Bogoslof Island.

Isosurfaces from later summer (Fig. 4E and F), when only seals were sampling, showed generalized warming at both 1 and 50 m, however the cold pool appeared to remain relatively stationary. Waters at 1 m around the Pribilofs increased to $\sim 7\text{--}8\text{ }^{\circ}\text{C}$ and the outer shelf west of St. George Island increased to $\sim 9\text{--}10\text{ }^{\circ}\text{C}$. The band of cool water at 50 m in the outer shelf persisted, however;

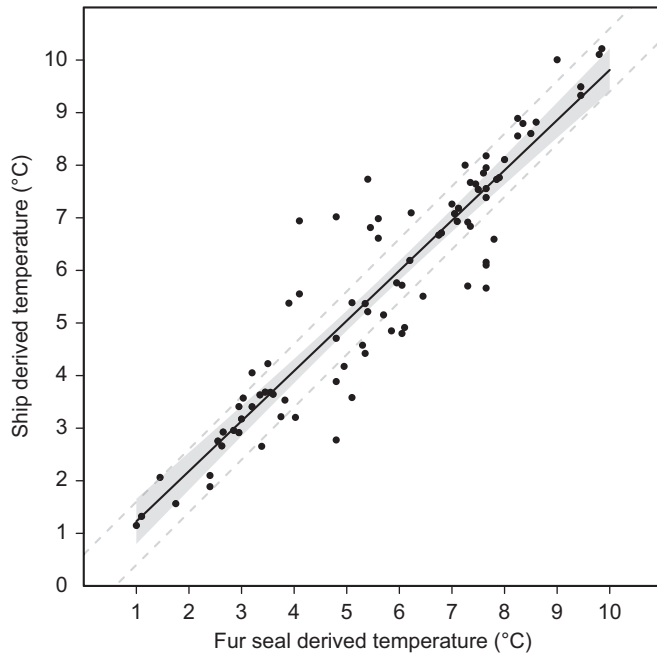


Fig. 3. Regression of temperature (°C) values collected at 1, 25, 50, 75, and 100 m by instrumented northern fur seals (when dives permitted) in relation to the nearest ship CTD cast within 10 km and 1 day (see Fig. 2.1C). Shading: 95% model confidence interval; gray dashed lines: ± 0.6 °C from 1 to 1 line (mean absolute difference between temperature pairings). There are 87 points comparing 32 stations/dives as collected by 20 individual fur seals.

it was less continuous as 4–5 °C water intersected it along the shelf-break.

3.4.2. Quantitative comparisons within surfaces

Results from DIVA cross-correlations (interpolated surface values correlated with observed temperature values) indicated a relative high-quality of fits ranging from 0.80 to 0.94 (where $\text{min}=0$ and $\text{max}=1$). Seal temperature surfaces at 1 m had better fits (July–August=0.89, August–September=0.94) than the 1 m ship surface while the ship surface fit was better (0.90) than the respective seal fits at 50 m (July–August=0.80, August–September=0.86). The July–August seal surfaces generated the highest (1 m field) and lowest (50 m field) statistical fits.

Isosurface error fields derived from ships and seals were notably different both in the distribution and the relative amount of error within the temperature surfaces (e.g. Fig. 5). Given that surfaces were masked, all resulting polygons were ringed with relatively large errors resulting from the cut-off at 0.25. The ship error field contained wide areas of relatively large errors (>0.20) and the surface itself was pocked with small zones where the errors exceeded the threshold (Fig. 5A). In contrast, seal error fields generally comprised contiguous areas of relatively low error (<0.10). Rare exceptions occurred in areas where the temperatures were interpolated between the southern limits of fur seal tracks from St. Paul Island and the northern extent of trips from Bogoslof Island (Fig. 5C and E) or in areas sampled by a lone fur seal. Overall, the ship surface had a greater degree of estimated error (median=0.08; Fig. 5B) compared to either seal surface (medians=0.02–0.03; Fig. 5C and F). Error fields were nearly identical at 1 m and 50 m highlighting the major role sampling distribution plays on mapping error.

3.4.3. Quantitative comparisons between surfaces

Extracted values from isosurfaces highlighted that both ship and seal maps tracked temperature changes across hydrographic

domains (Fig. 6). However, seal derived temperature estimates revealed finer details in the field compared to the smoothed estimates obtained from sparser ship data. The amount of error associated with the seal estimates was also noticeably less than ship estimates on both transects and at both 1 m and 50 m depths. Errors within transects from ship surfaces were not restricted to the terminuses, where increased error was expected as they coincided with the isosurface edge (due to the aforementioned error mask cutoff), but instead flared intermittently throughout the extracted length.

Difference surfaces highlighted areas where interpolated fields from ships and seals diverged (Fig. 7A and B) and summarized the magnitude of the discrepancies (Fig. 7C and D). Raw differences between 1 m surfaces ranged from -5.1 (where ship fields were cooler) to $+4.8$ °C (where ship fields were warmer) but 50% of the differences were within -0.17 and 1.13 °C (interquartile range). The largest raw differences occurred around St. George Island: (1) south along the 100 m isobath and over the Pribilof Canyon; (2) northeast on the 50 m plateau, and (3) west along the 200 m isobath (Fig. 7A). The raw differences approximated a normal distribution but overall the ship temperature surface was slightly warmer than the seal surface (median= 0.40 ± 1.14 °C).

Normalized differences between 1 m surfaces highlighted the inconsistencies remaining between temperature fields after attempting to account for the error within the respective ship and seal surfaces. Normalized differences between -1 and 1 indicated where fields were consistent within the estimated errors while differences < -1 (cooler) and > 1 (warmer) indicated where the fields were notably different. Half of the differences were within -0.17 and 1.23 (interquartile range) and again the ship surface was slightly warmer than seal surface (median= 0.36 ± 3.22). Large differences were again apparent around St. George coinciding with the previously described band of cooler water south and west of the island and with cooler but variable surface waters on the plateau of the Pribilof archipelago. Additionally, a narrow band north-east of Bogoslof Island was identified as a dissimilar zone (Fig. 7B).

3.5. Comparing vertical sections

Ship derived temperature cross-sections showed less detail and covered less area than those derived from seals (e.g. Figs. 8 and 9) in areas highly sampled by both platforms (Fig. 1D). Nonetheless, the cross-sections generated near Bogoslof Island (e.g. Figs. S1 and S2) and St. Paul Island tracked similar large scale shifts in the water column. For example, both ship (Fig. 8A) and seal (Fig. 8B) sections documented the abrupt transition from a weakly stratified 3-layer water column typical of the outer domain, to the strongly stratified 2-layer water column characteristic of the middle-domain (although the seal section was more informative thanks to increased sampling due east of St. Paul Island). Increased sampling by seals also made it possible to properly co-locate a shift in water column structure with the shelf-break south-west of St. Paul Island (Fig. 9B) as opposed to the same shift being documented more inshore on the outer shelf when using ship data (Fig. 9A). Had ships been sampling this area using a continuous transect (more traditional in physical oceanography), then the cross-sections would be more synoptic and the returned data would match the spatial scale of the survey design (but at the cost of being able to generate regional isosurfaces).

Fur seals documented the warming of the eastern Bering Sea in all hydrographic regions due to continued sampling following the end of the ship cruise (e.g. Figs. 8C and 9C). The sub-region bracketing St. Paul Island from east to west warmed unevenly in patches. On average, temperatures in the top 40 m increased over the outer shelf (mean= 0.61 ± 1.04 °C, $\text{max}=4.30$ °C), around St. Paul Island (mean= 1.06 ± 1.46 °C, $\text{max}=5.30$ °C) and over the

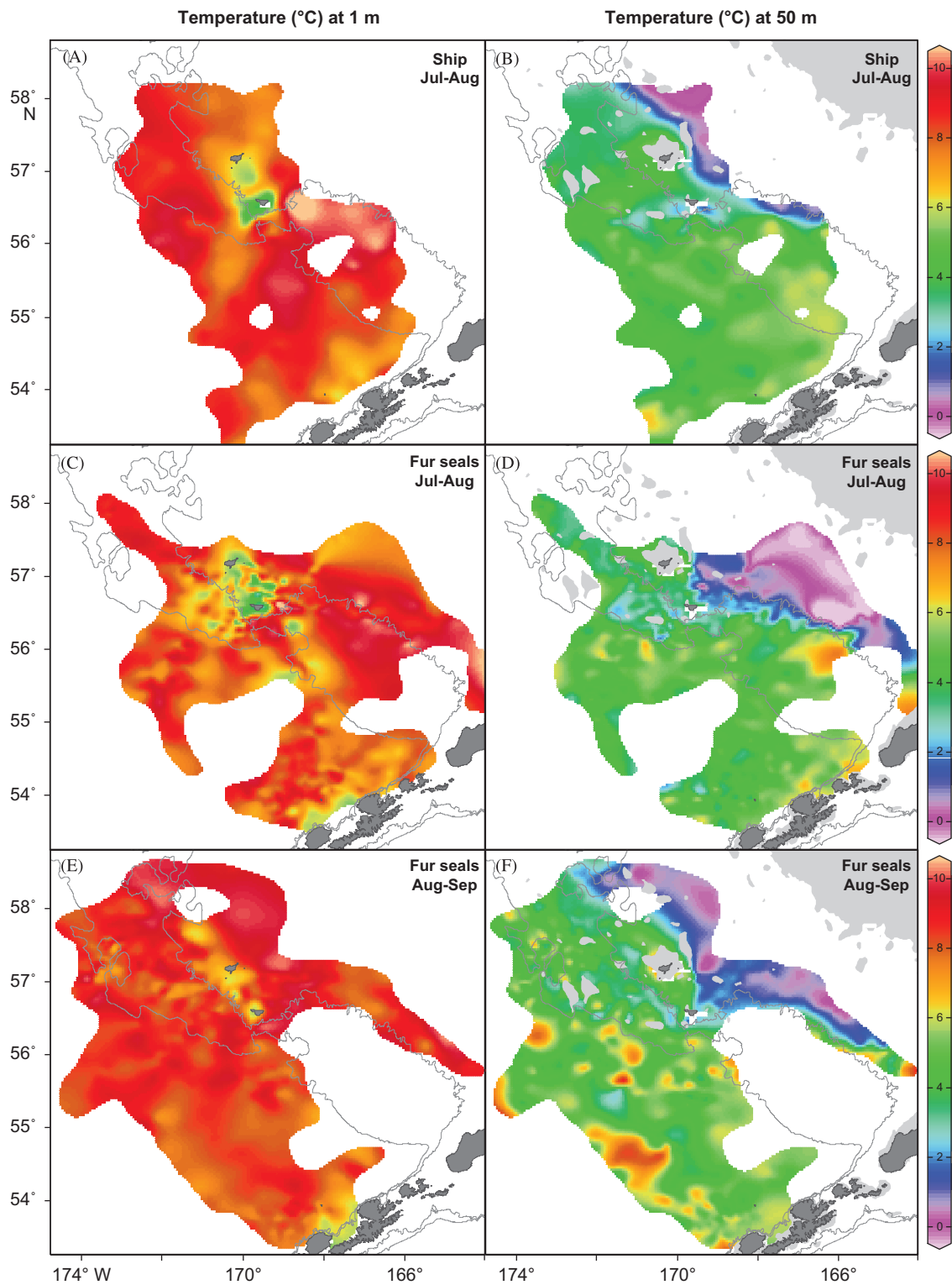


Fig. 4. Comparing interpolated temperature surfaces ($^{\circ}\text{C}$) of the eastern Bering Sea at 1m and 50m generated by ship CTD (panels A, B) or instrumented northern fur seal data (panels C, D) during July 15–August 15, 2009. Fur seals continued to collect data from August 16–September 17, 2009 (panels E, F).

middle shelf east of St. Paul Island to 167.25°W (mean = $1.56 \pm 1.84^{\circ}\text{C}$, max = 6.20°C) with the strongest changes typically occurring at the thermocline suggesting a deepening of the mixed layer (Fig. 8D). The region east of 167.25°W was not used in the domain average as the extreme cooling of the thermocline appears to be a sampling artifact, possibly the result of a limited number of seal dives at the outer limits of the delineated sub-region (Fig. 1D).

The sub-region intersecting the Bering Sea shelf and basin on a roughly north to south line also showed signs of warming with the most dramatic increases occurring on the outer shelf to depths of 100 m (mean = $1.7 \pm 1.11^{\circ}\text{C}$, max = 5.25°C ; Fig. 9D).

Seal dives over the basin south-west of St. Paul Island (Fig. 9B and C) occurred within a persistent anticyclonic eddy (Nordstrom et al., 2012; Paredes et al., 2012) and they recorded $\sim 7^{\circ}\text{C}$ water,

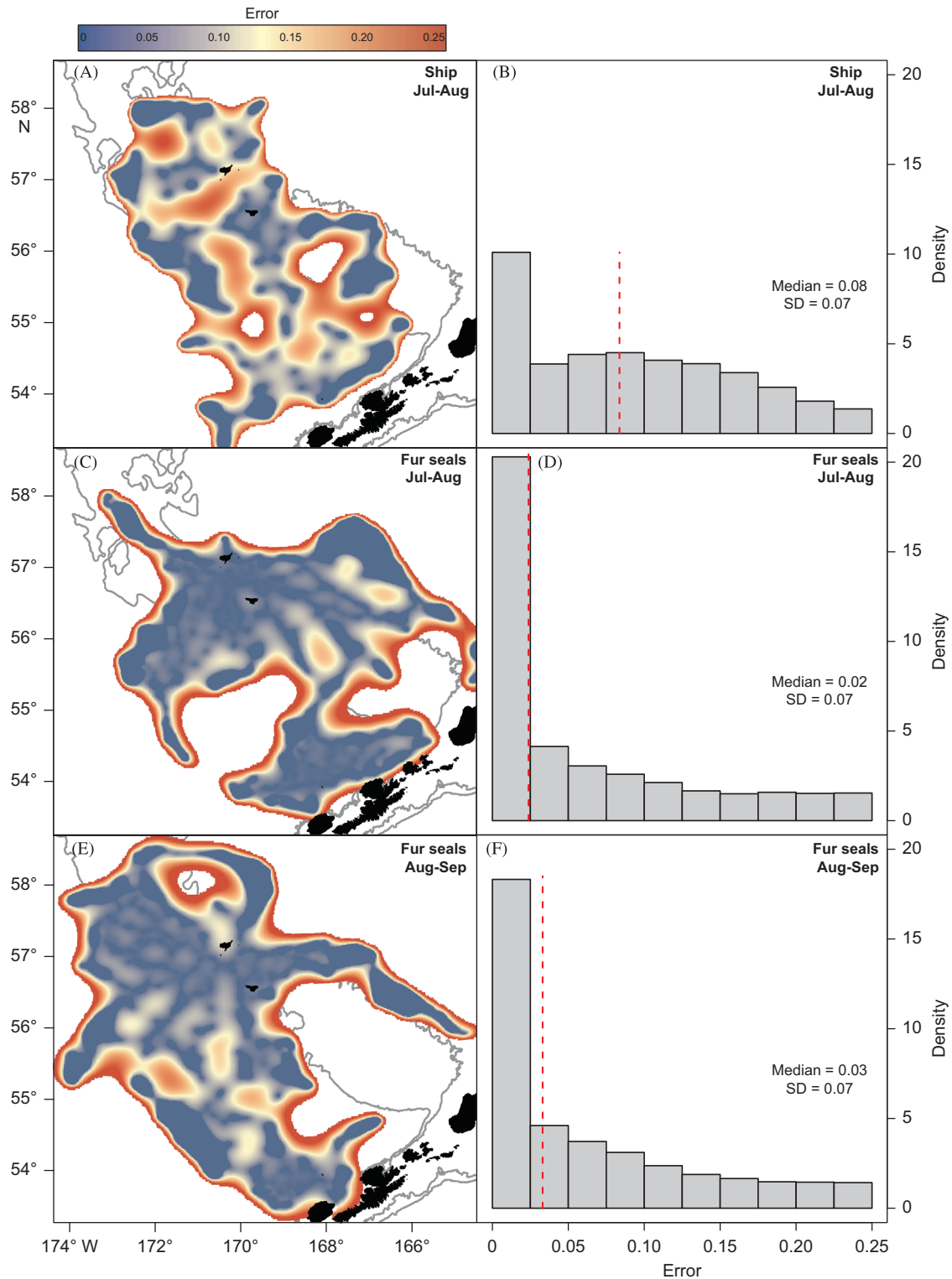


Fig. 5. Comparing temperature error fields in the eastern Bering Sea at 1m generated by ship CTD (panels A,B) or instrumented northern fur seal data (panels C,D) during July 15–August 15, 2009. Fur seals continued to collect data from August 16–September 17, 2009 (panels E,F). Median error levels of each surface are highlighted with a dashed line. Note: errors > 0.25 are masked from the analysis.

more typical of waters at 20 to 30 m depth, being drawn to the surface and segmenting the $\sim 9^\circ\text{C}$ surface waters from 55.5 to 56.25°N . The regularized, banded pattern was similar to the concentric ridges commonly observed in altimeter data (e.g., Fig. 1C) and was notable particularly during the July to mid-August period when the eddy was strongest. The same pattern was not detected using the coarser ship data (Fig. 9A).

3.6. Merged (ship and seal) isosurfaces

Given that temperature fields were similar at the regional scale, we integrated data collected by both platforms to produce isosurfaces that combined the sampling breadth of ships with the sampling resolution of fur seals (Fig. 10). Fine-scale temperature details were retained, and in some cases were enhanced, in the

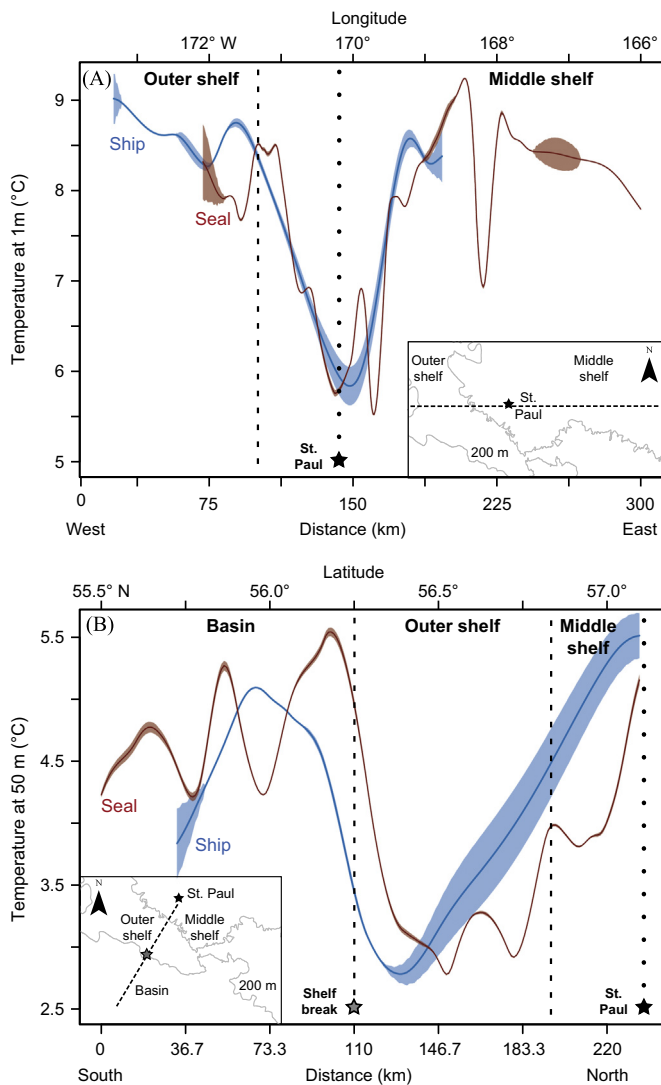


Fig. 6. Temperatures estimates (°C, solid lines) and associated errors (ribbons) extracted from July to August isosurfaces (Figs. 4 and 5) at 1 km intervals across the continental shelf of the eastern Bering Sea at 1 m depth (panel A) and from St. Paul I. south across the shelf-break to the basin at 50 m depth (panel B). Blue lines: ship derived surface; red lines: seal derived surface; dashed lines: isobath location; dotted line: St. Paul location. Isosurfaces were sampled along the mid-line of densely sampled sub-regions (insets, Fig. 1D i and ii). Note the relatively smoothed temperatures and wider-errors from ship-derived estimates compared to those from instrumented seals. (For interpretation of the references to color in this figure legend, the reader is referred to the web version of this article.)

resulting maps. For example, a cluster of CTD casts north of St. Paul Island linked previously disparate bands of ~ 2.5 °C water collected by fur seals on the east and west sides of the Pribilofs' (Fig. 4D) into a coherent ribbon surrounding the islands at 50 m (Fig. 10B). Those same casts better-defined the position of the cold-pool north of the Pribilof plateau.

Merged temperature maps also documented the cores of both anticyclonic and cyclonic eddies over the basin (Fig. 10). Anticyclonic (clockwise rotation) eddies commonly entrain warmer surface waters to deeper depths while cyclonic (counter-clockwise) eddies tend to transport colder water to the surface and this pattern has been documented in the southern Bering Sea (Mizobata et al., 2002) and the nearby Gulf of Alaska (Ladd et al., 2005). Temperature gradients at 1 m depth were too small in regional maps to adequately define these features from

temperature only (e.g. Fig. 10C); however, that was not the case at 50 m depth. A warm temperature anomaly near the center of the persistent eddy south-west of St. Paul Island was delineated (Fig. 10B i) as was an extension of the same feature that bordered the shelf-break farther east (Fig. 10B ii). Two cold temperature anomalies (assumed to be within cyclonic eddies) were also outlined over the central basin, albeit less sharply (Fig. 10B iii and iv). The temperature anomalies were confirmed as eddy cores by plotting the positions of encircling fronts which were derived from satellite altimeter measures of sea-surface height (Fig. 10D). Interestingly, plotting a simple sea-surface height anomaly for the same date places the temperature anomalies closer to eddy edges but this may be due to the lower spatial resolution of the coarser altimeter data. Nonetheless, it was possible to associate the temperature anomalies with sea-surface rotation for three of four eddies (Fig. 10B and D, i–iii), and in these cases the warm eddy cores were correctly associated with an anticyclonic rotation while the cold-core aligned with a cyclonic circulation. The fine-scale surface fronts did not perfectly enclose eddy cores although this was not to be expected given the fronts were highly dynamic and a single snapshot was overlaid on a month-long temperature composite.

4. Discussion

We used *in-situ* profiles, regional isosurfaces, error maps, difference surfaces, and vertical cross-sections to compare temperature data collected from ship-based CTDs with those collected by free-ranging, instrumented northern fur seals. Data from casts and dives relatively concurrent in time and space were similar as were regional temperature maps depicting well-described temperature structure in the eastern Bering Sea. Maps produced using fur seal data included more detail, less estimated error, and provided an additional 5-week period than those available from ship data generated with the study's sampling design. Maps produced using the integrated dataset preserved the fine-scale detail in the fur seal data while improving coverage due to the improved distribution of the ship stations, particularly north of St. Paul Island and over the basin. We propose that diving predators such as fur seals can provide high quality physical data products to support studies of their own ecology and to answer hydrographic questions provided that the instrumented species lend themselves to the questions of interest.

4.1. Comparing *in-situ* temperatures

Temperature profiles taken *in-situ* in a variety of hydrographic regions were strikingly similar regardless of whether thermistors were carried by ships or seals, particularly since the recordings could be separated by as much as 10 km and 24 h (e.g. Fig. 2). Relationships were similarly tight when ship derived temperatures were regressed against seal derived temperatures (Fig. 3). A nearly 1:1 relationship was found (slope=0.95) with only 13% error which suggested instrument performance was similar after binning temperature values to 1 m. Profiled readings between 4 and 8 °C were the most variable when compared likely because these temperatures were typical of the mid-water column where rapid shifts associated with the thermocline were more common and where temperature-depth pairings would be more affected than those well above or below the thermocline. Slight changes in the location and/or timing of the measurements, inherent to the paired ship casts and seal dives, likely contributed real temperature differences between sampling and would exacerbate instrument differences between readings.

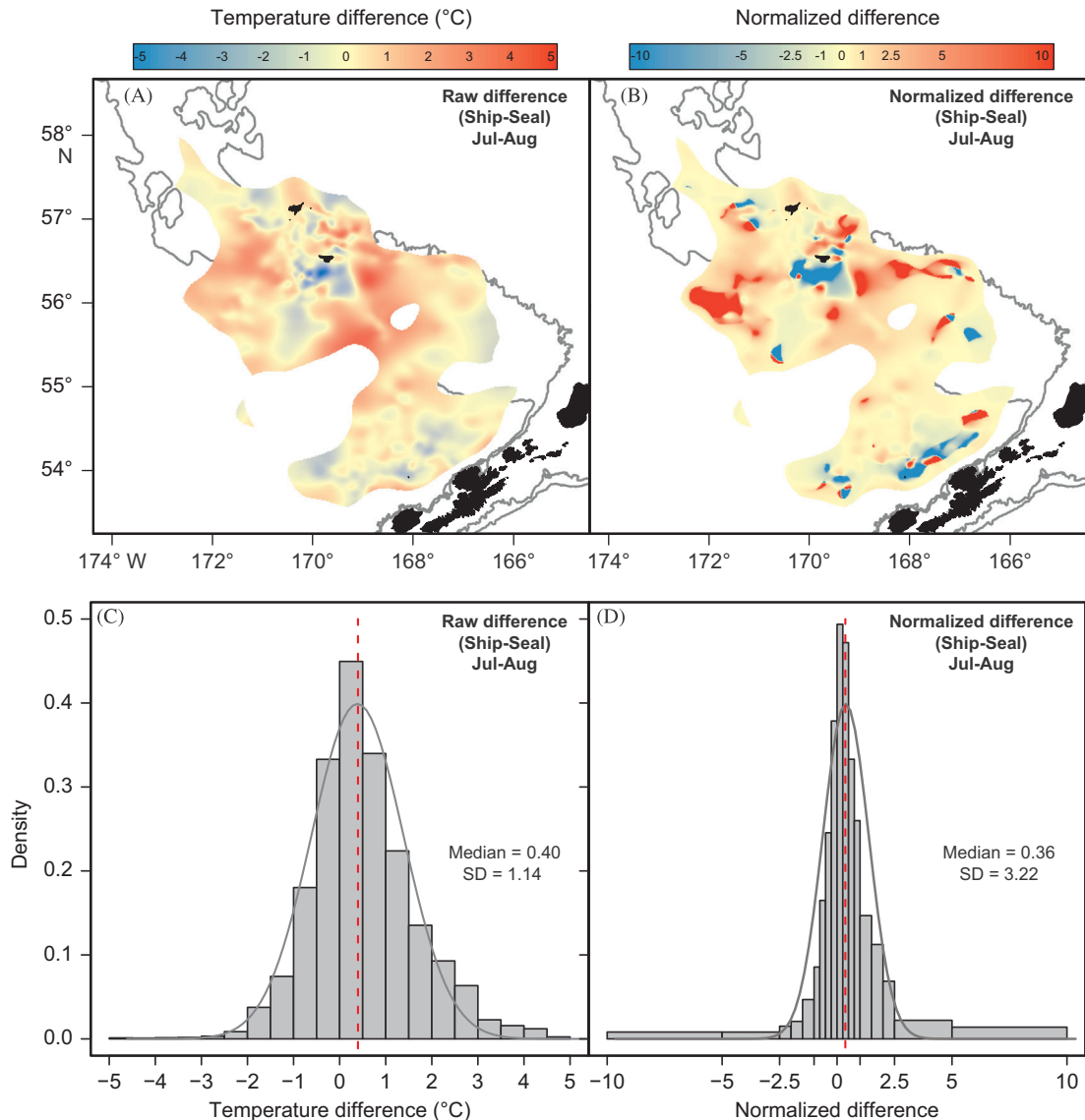


Fig. 7. Interpolated surfaces and histograms describing the differences between temperature fields generated at 1 m by ship CTD and instrumented northern fur seals in the eastern Bering Sea from July 15–August 15, 2009. Temperature ($^{\circ}\text{C}$) differences resulting from subtracting the seal surface (Fig. 4C) from the ship surface (Fig. 4A) are described in panels A and C while normalized differences (where temperature differences are corrected for error estimates) are depicted in panels B and D. Note: normalized differences between -1 and 1 indicate where fields are consistent within the estimated errors (yellows) and differences < -1 and > 1 indicated where the fields are notably different (blues and reds). (For interpretation of the references to color in this figure legend, the reader is referred to the web version of this article.)

4.2. Comparing temperature isosurfaces

Each surface polygon was the product of the correlation length, the specified error limit, and the sampling distribution. Correlation lengths and the error cut-off were kept consistent leaving the data coverage as the factor responsible for the different shapes and resolutions of the temperature surfaces. Regional maps were qualitatively similar where coverage was similar; however, fur seal isosurfaces revealed greater detail, particularly over the shelf region. For example, fur seals sampled the plateau between the Pribilofs intensively as they departed and returned to the rookery revealing chaotic, well-mixed surface waters in the early portion of the study followed by wide-spread warming up to 6°C in some areas as the summer progressed. Fur seals also traced a cool ($\sim 3^{\circ}\text{C}$) band of water along the 100 m isobath at 50 m depth that persisted throughout the study period. The band bifurcated east of St. George Island to surround the Pribilofs and may form part of a persistent front enveloping the islands (Kowalik and Stabeno, 1999; Sullivan et al., 2008) during summer months.

The benefits of high-resolution sampling were most apparent in areas that were highly physically dynamic. Given these areas typically coincided with known bathymetric features on-shelf, they are generally predictable and could be targeted in advance for additional study. Near-real time satellite altimetry and satellite-linked drifters have also been used successfully to direct detailed sampling in more pelagic environments (e.g., Ladd et al., 2005, 2012; Whitney and Robert, 2002). Future hydrographic work supporting upper trophic level studies, similar to the cruises in this study, could benefit from incorporating highly adaptive sampling schemes that would allow for additional casts or for towed CTD sampling in dynamic areas which would be akin to the fur seal sampling we observed in the study. Changes to physical sampling protocols could also be extended to net tows, acoustic sampling, or other biological collections to better describe relationships between prey and their environment at the finer scales at which predators commonly exploit them.

Goodness of fit and error estimates provided a quantitative assessment of the within surface variability for each individual

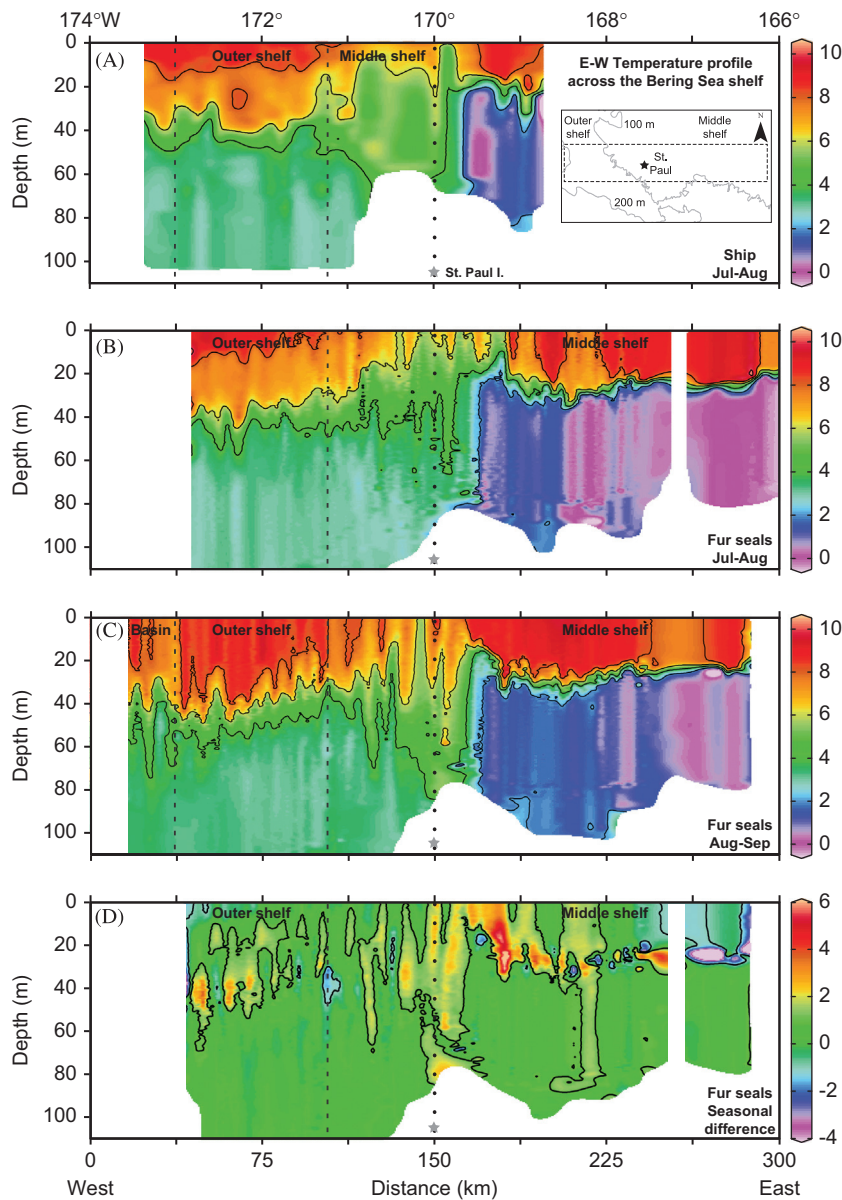


Fig. 8. Comparing interpolated temperature ($^{\circ}\text{C}$) cross-sections along a band across the eastern Bering Sea shelf bisecting St. Paul I. (see inset and Fig. 1D i) generated by ship CTD (panel A) or instrumented northern fur seals (panel B) from July 15 to August 15, 2009. Fur seals also collected data from Aug 16–Sep 17, 2009 (panel C) and the difference section (panel D) shows the patchy increase in temperature through to late summer in the upper 40 m of the water column (changes $> 1^{\circ}\text{C}$ are contoured in panel D). Dashed lines: isobath locations; dotted line: St. Paul location.

isosurface. The DIVA fit cross-correlation values have been shown to be overly optimistic for fields fit with the poor-man's error routine (Troupin et al., 2010) such as those used in this study but we restricted them to relative comparisons only. The error estimates within the interpolated temperature fields depended on two factors: the data coverage (again) and instrument error. The ship-board CTD's were more precise and more accurate instruments than the Mk-10 thermistors despite post-deployment corrections and limited sensor drift on the tags over time (Simmons et al., 2009). There was also more inherent variability within the 24 multi-purpose recorders deployed on seals than the two dedicated instruments deployed by the vessels. Given that error on data was negligible for ship instruments, the larger errors within the ship derived isosurfaces were primarily driven by their relatively limited sampling (Fig. 6).

High-resolution sampling by seals was also responsible for revealing finer temperature fluctuations (with less estimated error), than ship measures along identical transects extracted from temperature maps. The extracted data was predisposed to

contain less error than other areas of the maps as transects were placed along the center line of sub-regions previously identified as highly sampled areas for both platforms. Data extracted from alternative transects could show ships and seals as having similar temperature resolution and/or error rate depending on the placement. However, we observed subtle variations in temperature, an improved alignment of temperature with mapped isobaths, and limited error on the estimates in seal data both across the shelf near St. Paul Island (Fig. 6A) and across multiple domains (Fig. 6B) which were likely typical given the sheer number of seal samples in most areas.

The difference surfaces were difficult to interpret as the underlying sampling was not identical between ships and seals. Notable inconsistencies remained between the datasets despite 61% of the values in the normalized surface falling within -1 and $+1$ (indicating little difference). Outstanding differences could be related to the aforementioned instrument error of the tags, to sampling bias by fur seals, or to differences in the sampling time

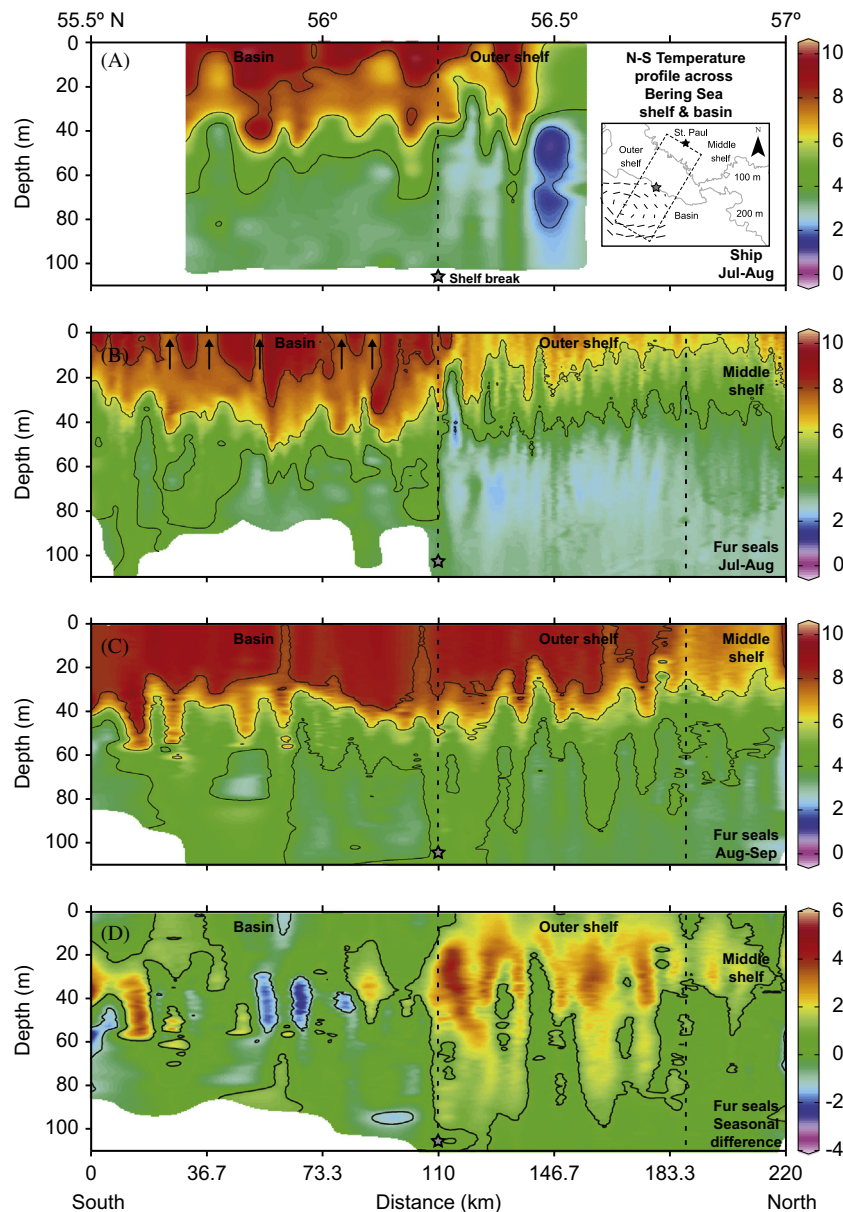


Fig. 9. Comparing interpolated temperature ($^{\circ}\text{C}$) cross-sections along a band from St. Paul I. (on-shelf) southwest to an area over the eastern Bering Sea basin within an eddy (see inset and Fig. 1D ii) generated by ship CTD (panel A) or instrumented northern fur seals (panel B) from July 15 to August 15, 2009. Fur seals also collected data from August 16–Sep 17, 2009 (panel C) and the difference section (panel D) shows the warming in the upper 40–60 m of the water column north of the shelf-break (located at $\sim 56.25^{\circ}$; changes $> 1^{\circ}\text{C}$ are contoured in panel D). Dashed lines: isobath locations; black arrows (panel B): temperature banding possibly due to concentric eddy currents.

of particular locations. Fur seal dives showed remarkable heterogeneity in their locations both between individuals and within seals tracked over multiple trips thereby limiting their sampling bias. Most discrepancies $\pm 3^{\circ}\text{C}$ were however, consistent with dynamic regions such as along isobaths, over canyons, and in areas of high vertical mixing (Fig. 7) which would be sensitive to differences in sampling time.

Both ships and seals detected spatial variability in temperature within dynamic areas at the regional scale but the specific boundaries placed by the spatial interpolations were strongly affected by the nearest casts or dives. Our composite maps (generated over a month) were presented as static snapshots but such temporally aggregated data would clearly mute dynamics occurring on a finer time scale which would be exacerbated in areas of rapid flux. The large inconsistencies remaining in the difference surfaces were not indicative of measures taken at the same time/locations (see Section 2.5.1

In-situ temperature comparisons) but rather we suspect they were the result of differences between predicted surfaces generated from datasets with very different spatial and temporal sampling strategies.

4.3. Comparing vertical sections

Seals recorded 4700 additional temperature profiles ≥ 50 m deep after the completion of the 5-week ship cruise which permitted us to examine sub-regions sampled most often at a finer-scale and over two time periods. The upper water column over much of the middle shelf, the waters surrounding St. Paul Island itself, and over the outer shelf experienced a warming and deepening of the mixed surface layer (e.g. Fig. 8B–D). Despite the lack of salinity measures, dramatic warming and increased structuring of the previously cooler and moderately mixed outer shelf waters was also documented south-west of St. Paul Island

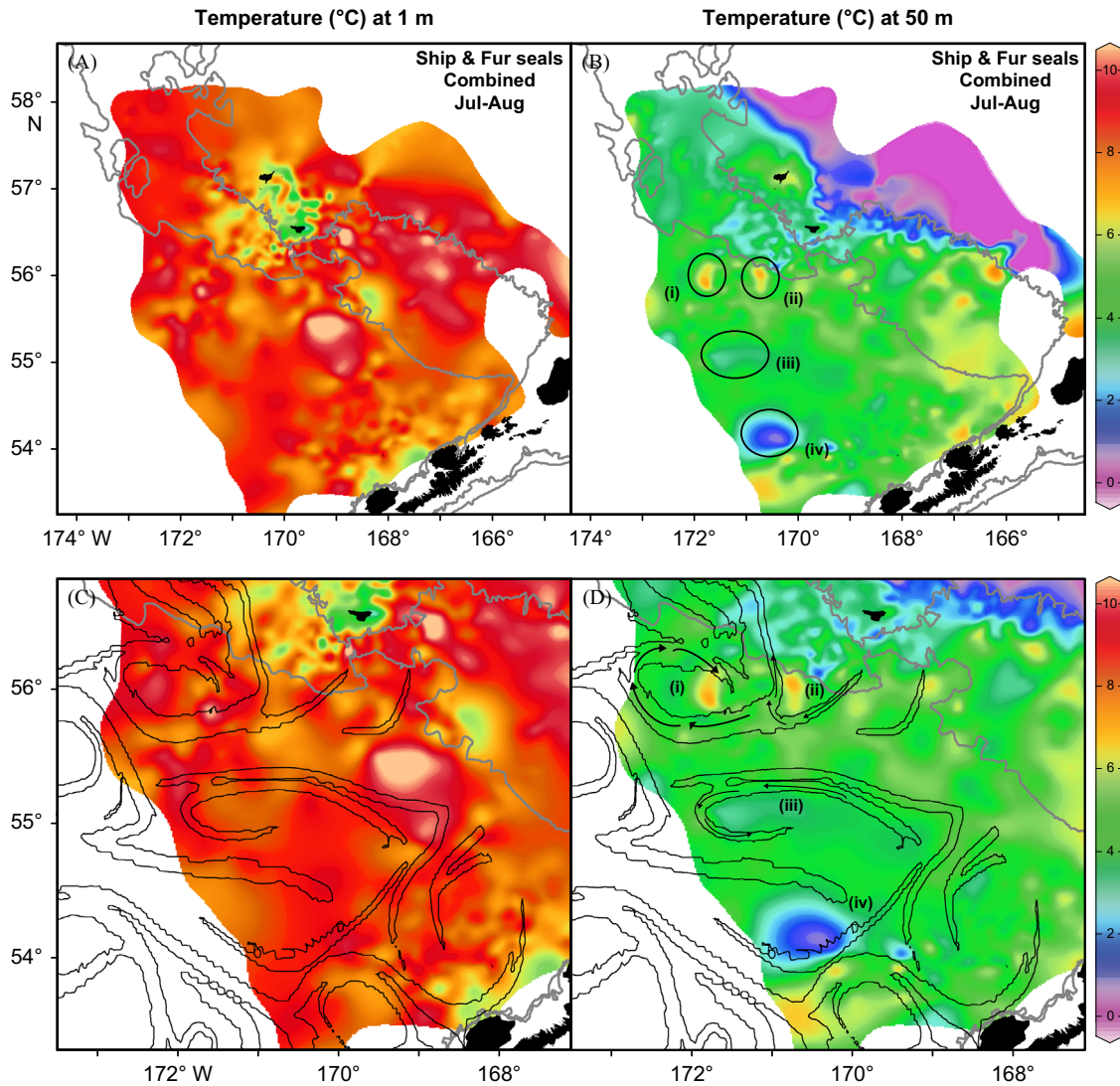


Fig. 10. Integrated temperature surfaces ($^{\circ}\text{C}$) of the eastern Bering Sea at 1 m (panels A and C) and 50 m (panels B and D) generated by combining and interpolating ship CTD data with instrumented northern fur seal data from July 15 to August 15, 2009. Contoured surface fronts (black lines, 0.2 FSLE/d) overlaid in panels C and D are derived from geostrophic current data from July 29, 2009. Anomalous warm and cold cores of confirmed anticyclonic (i, ii) and cyclonic (iii only) eddies are circled in panel B with rotational arrows added in panel D for emphasis.

(e.g. Fig. 9B–D). Fur seal derived observations agree with those from a recent study where the spatial distributions of stratification generally reflect the traditional boundaries of the middle and outer shelf domains (Ladd and Stabeno, 2012). However, the data were unique in that they track the development of stratification over a large area on the outer shelf and within the Pribilof domain as opposed to describing fully established stratification in the early fall.

Seals repeatedly sampled an anticyclonic eddy situated beyond the shelf-break and we suspect the temperature banding observed in the upper 20 m was indicative of concentric eddy currents drawing cooler waters to the surface (Fig. 9B). Spatial or temporal variability in the amalgamated seal dives could produce similar patterns to those observed, although the data in this area are generally synoptic as the sub-region coincides with a travel corridor from the rookery to the eddy and feeding trips averaged just over a week. However, we cannot confirm our suspicion without the density contours typically used to define eddies spanned in the Gulf of Alaska (Janout et al., 2009; Ladd et al., 2009, 2005). Similar temperature banding was not observed

within Bering eddies sampled on transects with stations > 10 km apart (Ladd et al., 2012; Mizobata et al., 2006), suggesting that finer scale CTD sampling, perhaps at 1 km intervals, would be required to detect such features from ships. The cooler intrusions were noted with less frequency and the upper 20 m was more homogenous (Fig. 9C) as the eddy core abutted the shelf break and began to wane in September.

Fur seals tracked temperature changes throughout the study period highlighting sometimes dramatic increases in specific locales. Longitudinal temperature records within a 2-month span (outside of mooring data) are relatively rare for most of the region as fisheries-based surveys rarely repeat transects. Recurring, short-term sampling of the basin, the slope, and even the outer shelf has been absent due to survey designs which are focused on the shallow continental shelf whereas moorings have been difficult to place in depths even approaching 200 m (but see Stabeno et al., 2009). The repeated measurements collected by fur seals across the region were therefore relatively unique and documented the continued warming of much of the eastern Bering, particularly the outer shelf waters to 100 m, over a relatively short span.

4.4. Merged (ship and seal) isosurfaces

The hybrid mapping approach using ships and seals appeared to balance the strengths and weaknesses of each data collection platform. Ship sampling locations could be chosen in advance within pre-defined regions creating a relatively well-distributed but small dataset to describe a large and varied oceanographic area. Fur seal sampling locations were entirely opportunistic (from a data collection perspective) but frequent dives from a large number of wide-ranging individuals created a large but occasionally clumped dataset describing the eastern Bering Sea. Merging data collected from ships and seals thereby produced temperature maps of the upper surface waters with an unparalleled combination of coverage and resolution, particularly beyond the 200 m isobath. Many studies have examined the water properties of the Bering Sea but have been typically confined to a limited area, feature, or transect. In contrast, the merged maps provided a contiguous view of some ephemeral summer processes as varied as the presence of the Pribilof front, the extent of the cold-pool, and the onset of stratification over the shelf while also delineating eddy cores over the basin.

Merging the ship and seal collected datasets provided the most complete temperature description of the region and highlights how traditional oceanographic measurements and animal-borne sampling can complement one another. For example, anomalous warm waters linked with anticyclonic eddies were evident at 50 m in the merged temperature record that were either poorly defined (seals only) or absent entirely (ships only) in the July–August isosurfaces derived from a single platform. Anomalous cold waters associated with cyclonic eddies were less defined as the surrounding waters were similarly cool and they were sampled less frequently resulting in a more diffuse definition of the core proper. In all cases, the addition of CTD profiles, taken in a more regular pattern over the basin, provided the missing data required to definitively isolate eddies from the background field. Supplemental ship-casts were not available, but were also less necessary to identify features over the basin during the August–September time period when fur seals increased their sampling in the area (e.g. Fig. 4F).

The observations we made from the merged regional maps were not novel and specific features may not have been recognized if not for the variety of oceanographic work previously conducted on smaller scales in various domains across the region. Well-mixed surface waters around the Pribilofs, the inner Pribilof front, the expansive cold-pool, and temperature domains delineated along major isobaths were all observed over the continental shelf while a high-degree of eddy activity was concurrently observed over the basin. The physical processes observed here all require continued dedicated study using a variety of *in-situ* and remote-sensing tools; however, the combination of ship and seal temperature data provided a unique snapshot of the processes at work across the whole of the southeastern Bering Sea and this hybrid approach may be applicable to a variety of oceanographic scenarios.

4.5. Considerations

Cost could be a determining factor when considering any combination of traditional and bio-logging data collection. While each situation will be unique, the operational costs of ship-sampling and fur seal sampling were very similar for this study. A range of financial assumptions were used in our estimates but cost differences were within 10% under any given scenario. Ship sampling involved fixed start-up costs but also high-constant operating costs (ship time fees) so the longer the sampling period, the greater the expense. In contrast, seal sampling also had fixed

startup costs (bio-logging instruments) but negligible operating costs. The comparisons only cover the overlapping 5-week sampling period from July–August 2009, after which ship costs would begin to outpace the expense required to maintain field crews. The disparity would continue to grow for multi-year sampling programs, even with the relatively high logistical costs of sub-polar field camps, as many times instruments can be recovered whereas ships must be re-chartered.

4.6. Limitations

The fast-response thermistor was the only oceanographic quality sensor onboard the fur seal borne packages which restricted the comparison with ships to temperature only. Ships carried a wide variety of instrumentation, thereby allowing them to sample additional physical and biological characteristics of the water column which can in turn help draw connections with other levels of the ecosystem, including top predators. Other tags exist that can alternatively include conductivity sensors or fluorometers (e.g. Sea Mammal Research Unit's CTD- SRDL) although their increased size restricts them to deployments on marine animals larger than small otariids such as female northern fur seals. Animal-borne sensors must also be minimized and hardened to withstand the rigors of the deployment which typically results in reduced sampling rates, response time, and resolutions.

Our study had a relatively large sample size (87 females) and the tagging effort focused on deployments that would maximize the spatial coverage at-sea yet there were areas that remained under sampled by fur seals. Obvious gaps included north of St. Paul Island and over the central basin, particularly in the July–August period. Deploying instruments on the northern rookeries would certainly improve sampling north of St. Paul Island as females there show high site fidelity to the shelf areas north of the island. In contrast, little could be done to improve central basin coverage as animals from Reef rookery (the study deployment site) typically forage over the central basin more than any other group of female fur seals. Female northern fur seals are known to be relatively shallow, nocturnal divers which limited their sampling primarily to the upper water column at night. Near surface (1 m) temperature recorded by the fur seals could therefore be slightly biased towards cooler values due to sampling after dark; however, a third of ship sampling was also conducted after sunset so discrepancies between isosurfaces were unlikely to have been driven by photoperiod. Sampling the upper 100 m was expected, but the number of fur seal dives deeper than 50 m decreased rapidly (n dives ≥ 75 m = 5620; ≥ 100 m = 2456) and became increasingly constricted to the outer shelf south of St. Paul Island. The comparisons we could make with ships and the extent to which we could describe the vertical structure of the Bering Sea was therefore limited. This was particularly evident for fur seals instrumented on Bogoslof Island as the majority of their dives were generally < 30 m. The physical limitations of the tags and the biological characteristics of the target species must be weighed alongside a project's goals and budget to determine whether bio-logging would be appropriate for any given application. In our case, a large number of northern fur seals were able to record a single environmental variable (temperature) extensively across a vast area and over an extended time period.

4.7. Conclusions and future research

Northern fur seals instrumented in the study collected high-quality temperature profiles at unprecedented spatial resolution in the upper water column of the eastern Bering Sea. They collected 26-times as many profiles as the ships over the same 5-week period and produced interpolated maps with finer detail

and less estimated error than similar surfaces produced by standard CTD casts. Inconsistencies between regional maps typically occurred in isolated clumps along isobaths or in high-mixing areas where subtle differences in the plotting of abrupt temperature shifts led to large differences in raw and normalized difference surfaces. Fur seals repeatedly sampled a range of hydrographic regions throughout their nursing period which tracked the continued warming of the upper water column in areas, such as the outer shelf, where longitudinal sampling within a season has been logistically challenging. Areas sampled intensively by fur seals were, by definition, biologically relevant areas to top predators and typically occurred where water masses mixed which were difficult to sample via ship. For example, some individuals repeatedly sampled temperatures within an anticyclonic eddy south-west of St. Paul Island and appeared to reveal subtle temperature intrusions associated with the eddy's concentric currents when the eddy was at peak strength. Integrated temperature maps simultaneously depicted phenomenon previously described in separate studies on-shelf or over the basin and therefore provided unbroken coverage over most of the region with high-resolution data clustered in dynamic areas.

Annual groundfish surveys collect hydrographic data according to a fixed grid across the majority of the eastern shelf and could be better informed about the finer-scale ocean characteristics between broadly spaced stations by incorporating data from free-ranging fur seals. Instrumenting animals from the north-east rookeries of St. Paul Island would provide the most value in that regard given their general fidelity to the shelf region. We recommend deploying multifunction instruments with environmental sensors in lieu of standalone time-depth recorders during future telemetry studies of northern fur seals whenever possible to increase the value of the data returned. In particular, sub-adult males have received little attention and their larger size would allow for deploying a complete CTD sensor suite (e.g., SMRU CTD-SRDL). Such a study would provide ecological insights into another sex class in addition to producing more informative hydrographic data.

Our animal-borne dataset benefitted by deploying a large number of instruments from two widely separated sources (*i.e.* rookeries) on a species with wide ranging foraging trips in order to match the vessels' sampling distribution and to compensate for the limited individual sampling at depths > 50 m. Northern fur seals also exhibited a high-dive frequency and were relatively non-selective in their foraging distribution at-sea (from a population sampling perspective). This produced a dataset with limited bias in terms of coverage which may not be true for other pinnipeds which show fidelity to highly specific areas (although these species would be well-suited to track changing oceanographic conditions in particular locales over time). Clearly, care must be taken to match the characteristics of potential instrument carriers with the data requirements in any bio-logging study. Our data show that hydrographic information collected by wide-ranging, diving animals such as fur seals can provide physical data products comparable to, and exceeding those provided by traditional sampling methods at regional or finer scales when the questions of interest coincide with the ecology of the species.

Acknowledgments

All animal procedures were conducted under the National Oceanographic and Atmospheric Administration (NOAA) permit no. 14,329 and abided by the guidelines of the Committee on Animal Care at the University of British Columbia (permit no. A09-0345). We thank S. Heppell, the captains, and the crews of

the *M/Vs Frosti* and *Goldrush* for their assistance in collecting the ship-board CTD data. We are also indebted to A. Baylis, J. Gibbens, R. Marshall, R. Papish, A. Will, and C. Berger for assistance with animal captures and instrument deployment. Thanks to A. Thomas for suggesting the Ocean Data View software used heavily in this work, to R. Pawlowicz for advice on comparing temperature fields, and to J.-M. Beckers for advice on accessing DIVA error estimates in ODV. C. Cotté calculated the FSLE for our study. Altimeter products were produced by Ssalto/Duacs and distributed by Aviso, with support from CNES. Two anonymous referees provided constructive criticism on an earlier version of the manuscript. This study was conducted as a part of the BEST-BSIERP "Bering Sea Project" funded jointly by the US National Science Foundation and the North Pacific Research Board. This is NPRB Publication Number 411 and BEST-BSIERP Bering Sea Project publication number 91.

Appendix A. Supplementary materials

Supplementary data associated with this article can be found in the online version at <http://dx.doi.org/10.1016/j.dsr2.2013.03.022>.

References

- Barth, A., Alvera-Azcárate, A., Troupin, C., Ouberdous, M., Beckers, J.-M., 2010. A web interface for gridding arbitrarily distributed *in situ* data based on Data-Interpolating Variational Analysis (DIVA). *Adv. Geosci.* 28, 29–37.
- Benoit-Bird, K.J., Kuletz, K., Heppell, S., Jones, N., Hoover, B., 2011. Active acoustic examination of the diving behavior of murrelets foraging on patchy prey. *Mar. Ecol. Prog. Ser.* 443, 217–235.
- Biuw, M., Boehme, L., Guinet, C., Hindell, M., Costa, D., Charrassin, J.B., Roquet, F., Bailleul, F., Meredith, M., Thorpe, S., Tremblay, Y., McDonald, B., Park, Y.H., Rintoul, S.R., Bindoff, N., Goebel, M., Crocker, D., Lovell, P., Nicholson, J., Monks, F., Fedak, M.A., 2007. Variations in behavior and condition of a Southern Ocean top predator in relation to *in situ* oceanographic conditions. *Proc. Natl. Acad. Sci., USA* 104, 13705–13710.
- Boehme, L., Meredith, M.P., Thorpe, S.E., Biuw, M., Fedak, M., 2008. Antarctic Circumpolar Current frontal system in the South Atlantic: monitoring using merged Argo and animal-borne sensor data. *J. Geophys. Res.* 113, C09012.
- Boffetta, G., Lacorata, G., Redaelli, G., Vulpiani, A., 2001. Detecting barriers to transport: a review of different techniques. *Phys. D: Nonlinear Phenom.* 159, 58–70.
- Boyd, I.L., Hawker, E.J., Brandon, M.A., Staniland, I.J., 2001. Measurement of ocean temperatures using instruments carried by Antarctic fur seals. *J. Mar. Syst.* 27, 277–288.
- Brasseur, P., Beckers, J.-M., Brankart, J.M., Schoenauen, R., 1996. Seasonal temperature and salinity fields in the Mediterranean Sea: climatological analyses of a historical data set. *Deep-Sea Res.* I 43, 159–192.
- Call, K.A., Ream, R.R., Johnson, D.S., Sterling, J.T., Towell, R.G., 2008. Foraging route tactics and site fidelity of adult female northern fur seal (*Callorhinus ursinus*) around the Pribilof Islands. *Deep-Sea Res.* II 55, 1883–1896.
- Campagna, C., Werner, R., Karesh, W., Marín, M.R., Koontz, F., Cook, R., Koontz, C., 2001. Movements and location at sea of South American sea lions (*Otaria flavescens*). *J. Zool.* 255, 205–220.
- Charrassin, J., Park, Y., Maho, Y., Bost, C., 2002. Penguins as oceanographers unravel hidden mechanisms of marine productivity. *Ecol. Lett.* 5, 317–319.
- Charrassin, J.B., Hindell, M., Rintoul, S.R., Roquet, F., Sokolov, S., Biuw, M., Costa, D., Boehme, L., Lovell, P., Coleman, R., Timmermann, R., Meijers, A., Meredith, M., Park, Y.H., Bailleul, F., Goebel, M., Tremblay, Y., Bost, C.A., McMahon, C.R., Field, I.C., Fedak, M.A., Guinet, C., 2008. Southern Ocean frontal structure and sea-ice formation rates revealed by elephant seals. *Proc. Natl. Acad. Sci., USA* 105, 11634–11639.
- Chilvers, B.L., Wilkinson, I.S., Duignan, P.J., 2005. Summer foraging areas for lactating New Zealand sea lions *Phocartos hookeri*. *Mar. Ecol. Prog. Ser.* 304, 235–247.
- Coachman, L.K., 1986. Circulation, water masses, and fluxes on the southeastern Bering Sea shelf. *Cont. Shelf Res.* 5, 23–108.
- Costa, D.P., Klinck, J.M., Hofmann, E.E., Dinniman, M.S., Burns, J.M., 2008. Upper ocean variability in west Antarctic Peninsula continental shelf waters as measured using instrumented seals. *Deep-Sea Res.* II 55, 323–337.
- d'Ovidio, F., Fernández, V., Hernández-García, E., López, C., 2004. Mixing structures in the Mediterranean Sea from finite-size Lyapunov exponents. *Geophys. Res. Lett.* 31, L17203.
- Gentry, R.L., 1998. Behavior and Ecology of the Northern Fur Seal. Princeton University Press, Princeton, New Jersey, U.S.A..

- Goebel, M.E., Bengtson, J.L., DeLong, R.L., Gentry, R.L., Loughlin, T.R., 1991. Diving patterns and foraging locations of female northern fur seals. *Fish. Bull.* 89, 171–179.
- Grist, J.P., Josey, S.A., Boehme, L., Meredith, M.P., Davidson, F.J.M., Stenson, G.B., Hammill, M.O., 2011. Temperature signature of high latitude Atlantic boundary currents revealed by marine mammal-borne sensor and Argo data. *Geophys. Res. Lett.* 38, L15601.
- Hunt Jr., G.L., Stabeno, P.J., 2002. Climate change and the control of energy flow in the southeastern Bering Sea. *Prog. Oceanogr.* 55, 5–22.
- Janout, M.A., Weingartner, T.J., Okkonen, S.R., Whitledge, T.E., Musgrave, D.L., 2009. Some characteristics of Yakutat Eddies propagating along the continental slope of the northern Gulf of Alaska. *Deep-Sea Res. II* 56, 2444–2459.
- Kowalik, Z., Stabeno, P.J., 1999. Trapped motion around the Pribilof Islands in the Bering Sea. *J. Geophys. Res.* 104, 25,667–625,684.
- Ladd, C., Crawford, W.R., Harpold, C.E., Johnson, W.K., Kachel, N.B., Stabeno, P.J., Whitney, F., 2009. A synoptic survey of young mesoscale eddies in the Eastern Gulf of Alaska. *Deep-Sea Res. II* 56, 2460–2473.
- Ladd, C., Kachel, N.B., Mordy, C.W., Stabeno, P.J., 2005. Observations from a Yakutat eddy in the northern Gulf of Alaska. *J. Geophys. Res.* 110, C03003.
- Ladd, C., Stabeno, P.J., 2012. Stratification on the Eastern Bering Shelf revisited. *Deep-Sea Res. II*. *in press*.
- Ladd, C., Stabeno, P.J., O'Hern, J.E., 2012. Observations of a Pribilof eddy. *Deep-Sea Res.* 1 66, 67–76.
- Lea, M.A., Guinet, C., Cherel, Y., Hindell, M., Dubroca, L., Thalmann, S., 2008. Colony-based foraging segregation by Antarctic fur seals at the Kerguelen Archipelago. *Mar. Ecol.-Prog. Ser.* 358, 273–287.
- Lydersen, C., Anders Nost, O., Kovacs, K.M., Fedak, M.A., 2004. Temperature data from Norwegian and Russian waters of the northern Barents Sea collected by free-living ringed seals. *J. Mar. Syst.* 46, 99–108.
- Mizobata, K., Saitoh, S.I., Shiomoto, A., Miyamura, T., Shiga, N., Imai, K., Toratani, M., Kajiwara, Y., Sasaoka, K., 2002. Bering Sea cyclonic and anticyclonic eddies observed during summer 2000 and 2001. *Prog. Oceanogr.* 55, 65–75.
- Mizobata, K., Wang, J., Saitoh, S.I., 2006. Eddy-induced cross-slope exchange maintaining summer high productivity of the Bering Sea shelf break. *J. Geophys. Res.*, 111.
- Nordstrom, C.A., Battaile, B.C., Cotté, C., Trites, A.W., 2012. Foraging habitats of lactating northern fur seals are structured by thermocline depths and submesoscale fronts in the eastern Bering Sea. *Deep-Sea Res. II* 51, 1033–1051.
- Okkonen, S.R., Schmidt, G.M., Cokelet, E.D., Stabeno, P.J., 2004. Satellite and hydrographic observations of the Bering Sea 'Green Belt'. *Deep-Sea Res. II* 51, 1033–1051.
- Paredes, R., Harding, A.M.A., Irons, D.B., Roby, D.D., Suryan, R., Orben, R.A., Renner, H., Young, R., Kitaysky, A., 2012. Proximity to multiple foraging habitats enhances seabirds' resilience to local food shortages. *Mar. Ecol. Prog. Ser.* 471, 253–269.
- R Development Core Team, 2009. *R: A language and environment for statistical computing*, 2.10.1 ed. R Foundation for Statistical Computing, Vienna, Austria.
- Resplandy, L., Lévy, M., d'Ovidio, F., Merlivat, L., 2009. Impact of submesoscale variability in estimating the air-sea CO₂ exchange: results from a model study of the POMME experiment. *Global Biogeochem. Cycles* 23, 017, GB1.
- Rixen, M., Beckers, J.-M., Brankart, J.M., Brasseur, P., 2000. A numerically efficient data analysis method with error map generation. *Ocean Modell.* 2, 45–60.
- Robson, B.W., Goebel, M.E., Baker, J.D., Ream, R.R., Loughlin, T.R., Francis, R.C., Antonelis, G.A., Costa, D.P., 2004. Separation of foraging habitat among breeding sites of a colonial marine predator, the northern fur seal (*Callorhinus ursinus*). *Can. J. Zool.* 82, 20–29.
- Roquet, F., Charrassin, J.-B., Marchand, S., Boehme, L., Fedak, M., Reverdin, G., Guinet, C., 2011. Delayed-mode calibration of hydrographic data obtained from animal-borne satellite-relay data loggers. *J. Atmos. Oceanic Technol.* 28, 787–801.
- Roquet, F., Park, Y.-H., Guinet, C., Bailleul, F., Charrassin, J.-B., 2009. Observations of the Fawn Trough Current over the Kerguelen Plateau from instrumented elephant seals. *J. Mar. Syst.* 78, 377–393.
- Schlitzer, R., 2011a. *Ocean Data View 4.4.1* <<http://odv.awi.de>>, 27568 Bremerhaven, Germany.
- Schlitzer, R., 2011b. *Ocean Data View 4.4.1 User's manual*, 27568 Bremerhaven, Germany.
- Schumacher, J.D., Stabeno, P.J., 1994. Ubiquitous eddies in the eastern Bering Sea and their coincidence with concentrations of larval pollock. *Fish. Oceanogr.* 3, 182–190.
- Simmons, S., Tremblay, Y., Costa, D., 2009. Pinnipeds as ocean-temperature samplers: calibrations, validations, and data quality. *Limnol. Oceanogr.: Meth.* 7, 648–656.
- Simmons, S.E., Crocker, D.E., Hassrick, J.L., Kuhn, C.E., Robinson, P.W., Tremblay, Y., Costa, D.P., 2010. Climate-scale hydrographic features related to foraging success in a capital breeder, the northern elephant seal *Mirounga angustirostris*. *Endangered Species Res.* 10, 233–243.
- Sinclair, E.H., Vlietstra, L.S., Johnson, D.S., Zeppelin, T.K., Byrd, G.V., Springer, A.M., Ream, R.R., Hunt Jr., G.L., 2008. Patterns in prey use among fur seals and seabirds in the Pribilof Islands. *Deep-Sea Res. II* 55, 1897–1918.
- Stabeno, P.J., Bond, N.A., Kachel, N.B., Salo, S.A., Schumacher, J.D., 2001. On the temporal variability of the physical environment over the south-eastern Bering Sea. *Fish. Oceanogr.* 10, 91–98.
- Stabeno, P.J., Kachel, N., Mordy, C., Righi, D., Salo, S., 2008. An examination of the physical variability around the Pribilof Islands in 2004. *Deep-Sea Res. II* 55, 1701–1716.
- Stabeno, P.J., Ladd, C., Reed, R.K., 2009. Observations of the Aleutian North Slope Current, Bering Sea, 1996–2001. *J. Geophys. Res.* 114, C05015.
- Stabeno, P.J., van Meurs, P., 1999. Evidence of episodic on-shelf flow in the southeastern Bering Sea. *J. Geophys. Res.* 104, 29715–29720.
- Sterling, J.T., 2009. *Northern fur seal foraging behaviors, food webs, and interactions with oceanographic features in the eastern Bering sea*. School of Aquatic and Fishery Sciences. PhD Thesis, University of Washington, Seattle, p. 233.
- Sullivan, M.E., Kachel, N.B., Mordy, C.W., Stabeno, P.J., 2008. The Pribilof Islands: Temperature, salinity and nitrate during summer 2004. *Deep-Sea Res. II* 55, 1729–1737.
- Trathan, P.N., Green, C., Tanton, J., Peat, H., Poncet, J., Morton, A., 2006. Foraging dynamics of macaroni penguins *Eudyptes chrysolophus* at South Georgia during brood-guard. *Mar. Ecol. Prog. Ser.* 323, 239–251.
- Tremblay, Y., Shaffer, S.A., Fowler, S.L., Kuhn, C.E., McDonald, B.I., Weise, M.J., Bost, C.-A., Weimerskirch, H., Crocker, D.E., Goebel, M.E., Costa, D.P., 2006. Interpolation of animal tracking data in a fluid environment. *J. Exp. Biol.* 209, 128.
- Troupin, C., Machín, F., Ouberdous, M., Sirjacobs, D., Barth, A., Beckers, J.-M., 2010. High-resolution climatology of the northeast Atlantic using data-interpolating variational analysis (DIVA). *J. Geophys. Res.* 115, C08005.
- Troupin, C., Barth, A., Sirjacobs, D., Ouberdous, M., Brankart, J.-M., Brasseur, P., Rixen, M., Alvera-Azcárate, A., Belounis, M., Capet, A., Lenartz, F., Toussaint, M.-E., Bekers, J.-M., 2012. *Ocean Modell.* 52–53, 90–101.
- Weise, M.J., Harvey, J.T., Costa, D.P., 2010. The role of body size in individual-based foraging strategies of a top marine predator. *Ecology* 91, 1004–1015.
- Whitney, F., Robert, M., 2002. Structure of Haida eddies and their transport of nutrient from coastal margins into the NE Pacific Ocean. *J. Oceanogr.* 58, 715–723.